NOAA Technical Memorandum NOS OMA 13

ANALYSIS OF CIRCULATION CHARACTERISTICS IN THE VICINITY OF DEEPWATER DUMPSITE 106

Dr. Charles N. Flagg, Mr. Daniel E. Frye,
Mr. Peter R. Daifuku

EG&G WASC Oceanographic Services
77 Rumford Avenue
Waltham, Massachusetts 02154

Rockville, Maryland
February 1985

UNITED STATES
DEPARTMENT OF COMMERCE
Malcolm Baldrige, Secretary

National Oceanic and
Atmospheric Administration
Anthony J. Calio,
Deputy Administrator

National Ocean Service
Paul M. Wolff,
Assistant Administrator

Prepared by

EG&G WASC Oceanographic Services
77 Rumford Avenue
Waltham, Massachusetts 02154

for the

Coastal and Estuarine Assessment Branch
Ocean Assessments Division
Office of Oceanography and Marine Assessment
National Ocean Service
National Oceanic and Atmospheric Administration
U.S. Department of Commerce

NOTICE

CONTENTS

FIGURES

TABLES

Analysis of Circulation Characteristics in the Vicinity of Deepwater Dumpsite 106

Dr. Charles N. Flagg
Mr. Daniel E. Frye
Mr. Peter R. Daifuku

ABSTRACT. More than 300 months of current meter data have been analyzed to describe the long-term mean circulation patterns found in the offshore slope region along the U.S. East Coast. The general pattern of slope circulation, based on monthly averaged data over a span of 14 years, consists of a downcoast drift parallel to the isobaths toward the west and southwest. This mean current system extends throughout the water column and across the width of the slope water region from the shelf break to at least 150 km offshore. The westward to southwestward drift is strongest in the near-surface layer above the main thermocline (above 200 meters). Mean current speeds are variable at these shallow depths, but are typically in excess of 10 cm/sec. Current direction is also variable near the surface, resulting in a complex vertical current structure. The major source of this variability is the occurrence of warm core rings. Seasonal patterns are not readily observed in the slope currents except near the surface where a small annual signal can be detected in the background current field; i.e., in the absence of warm core rings. An attempt to relate this to the local wind stress was unsuccessful, but the possibility remains that the variation may still be attributable to atmospheric forcing on a larger scale. On time scales shorter than one month, considerable variability is seen in both the speed and direction of the background currents. Fluctuations are normally polarized in a direction parallel to the local isobaths; however, on-shelf currents occur with a frequency of roughly 15% and persist for periods of days to weeks. Short-term recirculation events are, apparently, quite rare. Low current speed events, e.g., below 5 cm/sec, are observed on an infrequent basis (~10%), and generally do not persist for periods of more than two days.

1. INTRODUCTION

1.1 Site Description

The 106-Mile Deepwater Dumpsite (DWD 106) covers a rectangular area of roughly 1500 square kilometers located between latitude 38°40'N and 39°00'N and longitude 72°00'W and 72°30'W. The site is centered at a point 106 miles southeast of Ambrose Light and is convenient to the major ports along the U.S. mid-Atlantic coast. In relation to bottom topography, the site lies just beyond the seaward limit of the continental shelf (200-meter isobath) and covers a portion of both the continental slope and the continental rise. Depths vary between 1700 and 2750 meters within the dumpsite boundaries.

At present, the site is used for the regulated dumping of industrial wastes under management of EPA Region II. The volume of waste material involved has been dramatically reduced since 1972 when EPA was granted the authority to regulate ocean disposal activities under the Marine Protection, Research, and Sanctuaries Act. Despite the recognized environmental risks, it is likely that the present level of dumping activity at the site will continue into the foreseeable future due to the lack of preferable land-based disposal options for certain industrial wastes. Also for this reason, the possibility exists for increased usage of the site under more relaxed regulatory restrictions. This outlook warrants a concentrated effort toward an increased understanding of the oceanic environment and the factors that determine the fate of pollutant discharges. In particular, this report is concerned with the problem of describing the mean current characteristics of the site and of the slope water region in general in order to provide an accurate account of the role of advective processes in determining the fate of pollutants.

Three distinct oceanographic regimes characterize the surface waters in the vicinity of the dumpsite: shelf water, slope water, and Gulf Stream water. Shelf water lies inshore of the shelf water/slope water front which is generally found approximately over the shelf break. The slope water occupies the region between this front and the north wall of the Gulf Stream. The position of this boundary is highly variable and may intrude inshore virtually to the shelf. Normally, the Gulf Stream is found along the lower portion of the continental rise, so that the dumpsite is contained within the slope water region. Consequently, the slope water is of major interest, including both the physical and chemical characteristics and the dynamic features comprising its various circulatory characteristics.

1.2 Objectives

The present report focuses on questions relating to the nature of long-term advective processes, particularly with regard to the mean circulation patterns in the near-surface layer above the seasonal thermocline where certain industrial wastes are likely to be trapped by the density structure. The deeper currents are also of interest, since future dumping may include heavier materials which would fall through the seasonal and/or permanent thermocline. An examination of the specific effects of warm core rings on waste dispersion is not an objective of this study, but the effects of warm

core rings on current statistics are considered as part of the overall data analysis task.

The collected data describing the general circulation patterns in the slope region are used to characterize specific advective features at DWD 106 in terms of their probability of occurrence. These include residence times of waters within DWD 106 and within the slope region, recirculation via low-frequency current reversals, and the incidence of near-stagnant conditions at DWD 106 or rapid on-shelf motions. Finally, the ultimate or long-term fate of waters passing through DWD 106 is considered by means of an examination of the data for evidence of a large-scale gyre or recirculation mechanism which could lead to the long-term accumulation of certain pollutants in the slope water region.

This study summarizes the collective data base available from long-term current measurements using internally recording instruments and drifting buoys. While the results obtained may not be complete or unambiguous, they do reflect an examination of the bulk of current data collected on the slope between 1968 and 1981. Recent studies performed by the Minerals Management Service and others will undoubtedly bring new information and new conclusions to the description of the general circulation patterns in this area.

2. OCEANOGRAPHIC BACKGROUND

2.1 General Physiography

The slope waters off the U.S. East Coast occupy an oceanographically distinct region (Iselin, 1936) bounded on the west by the shelf/slope front and on the east by the Gulf Stream. In the alongshore direction, the region stretches from Cape Hatteras to the Grand Banks, covering an area of about 180,000 km^2, depending upon the position of the Gulf Stream. Within this area, the bottom depth increases from 200 to over 4000 meters so that the volume of slope water is approximately 650,000 km^3. It is a dynamically active region subject to massive incursions of Sargasso water due to Gulf Stream meanders, mixture with shelf water in the upper 200 meters or so, and occasional intrusions from the northeast of large amounts of cold Labrador Sea water at mid-depth. It is also an area of significant topographic Rossby wave energy. The following paragraphs give a brief summary of the research in the slope waters and outline the physical properties and dynamics of the region as we understand them.

2.2 Hydrography

Wright (1977), in his review of the water masses of the slope region, divides the water column into three layers. The upper 200 meters contain the waters that interact with the atmosphere and undergo a significant annual variation. It is also within this region that the influence of the fresher shelf waters is seen. The charts of surface temperature compiled by Schroeder (1966) indicate that in the winter there is a very strong horizontal thermal gradient of about 15°C across the slope waters from the northern wall of the Gulf Stream to the shelf break. In summer, this temperature contrast

decreases substantially as the surface layers over the shelf and slope are warmed so that, on average, there is only a 5°C decrease from the Gulf Stream to the shelf. In both the summer and winter, the mean isotherms in the upper layer parallel the mean course of the Gulf Stream. The vertical temperature distribution in the upper layer tends to be nearly isothermal during the winter season. A weak, shallow thermocline, over a depth range from 10 to 40 meters, tends to develop from late spring to early fall. This structure is vulnerable to mesoscale processes and energetic meteorological events.

The influence of shelf water is produced by complex exchange processes across the shelf/slope water boundary. This boundary has a mean position in the vicinity of the shelf break, but undergoes substantial onshore-offshore excursions on a wide range of time scales. During the colder months, when the surface temperature contrast between the two water masses is particularly strong, the boundary appears as a discontinuous front in infrared satellite imagery. The interface is generally inclined to the vertical, with the shelf water extending seaward as an overlying wedge of colder, fresher water. Mixing processes along this front are complex, being dependent on wind conditions and the influence of Gulf Stream meanders (see below). The surface temperature contrast is reduced during the summer months, but a strong gradient may remain at depths below 100 meters. As reported by Bumpus (1976) and others, temperatures between 6°C and 8°C are often found in the lower portion of the water column along the outer shelf. This "cold pool" is initially composed of remnant winter shelf water and subsequently maintained by a flow of water from intermediate depths in the Gulf of Maine (Flagg, 1984). There is good evidence that it flows southward along the 200-meter isobath during the summer months and is eventually entrained in the Gulf Stream east of Cape Hatteras (Boicourt, 1973). Alternatively, some of the cold pool may move offshore and become entrained as a "bubble" in the slope water. Inshore intrusions of slope water at mid-depth along the shelf break have also been widely observed.

The seaward boundary of the slope water region, known as the north wall of the Gulf Stream, is conventionally defined by the position of the 15°C isotherm at a depth of 200 meters. This boundary is highly variable (Hansen, 1970), but its mean position lies roughly along the lower continental rise near the 4000-meter isobath.

The salinities of the upper layer of the slope water appear to be as variable as temperature, but with a smaller range. The salinities in the slope region typically range from about 34.8 ppt just offshore of the shelf/slope front, to somewhat more than 36 ppt at the boundary with Gulf Stream water. In these waters, it is common to find a salinity maximum layer having values of about 35.5 ppt between 100 and 200 meters. This is especially noticeable along the shelf break where the fresher shelf water has mixed with slope water near the surface.

At 200 meters, there is little annual temperature variability. Temperatures at this depth decrease uniformly from about 18°C in the Sargasso to somewhat less than 11°C along the shelf west of Cape Sable (Schroeder, 1963). Colder water is found east of this point, reflecting the influence of water from the Labrador Sea (Gatien, 1976).

The second layer in the slope water identified by Wright (1977) is the main (permanent) thermocline, which extends from about 200 to 500-600 meters. The bottom of the thermocline is typically marked by the 5°C isotherm, which is found about 700 meters shallower in the slope region than in the central Atlantic (Fuglister, 1963). Salinity decreases from approximately 35.5 ppt at 200 meters to about 35.0 ppt at about 600 meters.

The third layer in the slope water is the deep region from about 500 meters to 4000 meters or more, where the vertical gradients of temperature and salinity are small. Temperature below the thermocline decreases to approximately 2°C near the bottom while salinity undergoes a change of less than 0.1 ppt. Wright (1977) summarizes the evidence which indicates that three distinct water masses, all of northern origin, reside within the lower layer.

2.3 Circulation

The synoptic current characteristics of the slope region have only been defined in their roughest outline even though there have been some high-quality current measurements performed in the region. The best information on currents is obtained from moorings deployed along the inshore edge of the region; e.g., Site D (Webster, 1969). The major current feature of the region, at least in the upper layers, is a westward drift between the shelf edge and the Gulf Stream. Surface currents originate as the Labrador Current, which sweeps around the Grand Banks, continues along the edge of the shelf in a wide and diffuse stream, and finally turns sharply eastward near Cape Hatteras as it joins the Gulf Stream. The current system in the vicinity of the Grand Banks is quite complex and has been studied intensely (McLellan, 1957; Swallow and Worthington, 1961, 1969; and Clarke et al., 1980), but direct evidence for a continuous westward flow is weak, even though the water property distribution requires that there be such a flow.

A complete dynamical explanation for the southwesterly surface current in the slope region is not entirely clear. The current is at least partially related to the curl of the wind stress produced by north-south variations in the mean zonal winds combined with a general strengthening of the easterly wind stress with distance offshore. This mechanism suggests that the southwesterly flow may be an expression of a large-scale anticyclonic circulation occupying the entire slope water region. This circulation may or may not form a closed gyre. Evidence for such a feature is provided by numerical modeling experiments of the Gulf Stream system (Semtner and Mintz, 1977; Beardsley and Winant, 1979) which incorporate realistic bathymetry along the continental margin and the effect of zonal wind stress variations. These results also indicate the presence of an alongshore pressure gradient at the shelf break. Such a pressure gradient had been postulated by several investigators (Scott and Csanady, 1976; Csanady, 1977) as the only possible means to drive the alongshore flow observed over the shelf in opposition to the mean eastward wind stress. Local driving forces, such as winter storms and freshwater runoff, also contribute to the alongshore flow inshore of the shelf break. However, recent theoretical evidence (Csanady and Shaw, 1983) indicates that such driving forces do not extend offshore to the slope region due to the insulating effect of the steep bottom slope, particularly for depths below the main thermocline.

The southwesterly flow over the shelf appears to be derived from water originating in the Gulf of Saint Lawrence, while the alongshore surface flow within the slope region appears to be an extension of the Labrador Current. The slope water achieves its distinctive characteristics by virtue of mixing with Scotian Shelf water along its inshore boundary and, to a greater extent, with Gulf Stream and Sargasso water along its seaward boundary. Both processes appear to be regulated by the influence of anticyclonic warm core rings. Isotopic data suggest that mixing across the shelf/ slope boundary along the mid-Atlantic Bight is less intense (Fairbanks, 1982).

In the deep water of the slope region, the major current feature is the Western Boundary Undercurrent, which is ultimately supplied with water from the Norwegian Sea overflow (Warren, 1981). The flow of this water around the Grand Banks has been documented by Swallow and Worthington (1961, 1969) using Swallow floats, and it is estimated that the transport of this water is about 10 to 20 x 10^6 m^3/sec. The Western Boundary Undercurrent flows along the continental rise and leaves the slope area by flowing beneath the Gulf Stream off Cape Hatteras (Richardson, 1977).

Warm core rings and meanders of the Gulf Stream strongly perturb the mean circulation patterns in the slope region (Saunders, 1971; Gotthardt and Potocsky, 1974). These warm core rings may have orbital velocities as high as 2 knots or more, extending to depths of more than 1000 meters (EG&G, 1978). Temperatures and salinities associated with the rings can be radically different from the surrounding slope waters. When they encounter the shelf/slope front, vast quantities of fresh/cold shelf water are sometimes drawn off the shelf and eventually absorbed into the slope water (EG&G, 1982). There is a major research program presently being carried out to better understand the effect of warm core rings (Kester, 1981), but it is clear from their frequency of occurrence and their current and property anomaly fields that the effect is great.

The aspect of the slope water currents that has attracted the greatest amount of attention is the low-frequency wave motion with typical amplitudes on the order of 10 cm/sec and periods within the range from roughly 8 to 20 days. This motion is explained by the theory of topographic Rossby waves (Rhines, 1970) which are generated by deep fluctuations in the Gulf Stream. Initially, the waves propagate westward as barotropic Rossby waves over the deep oceanic region beneath the Gulf Stream, but are then transformed to bottom-trapped, topographic Rossby waves as they travel over the rise and slope regions (Hogg, 1981). This produces an amplitude intensification with depth. Hamilton (1982) has shown the significance of these waves in analyzing the data collected from a near-bottom array of current meters at the 2800-meter radioactive dumpsite located roughly 30 kilometers south-southeast of DWD 106. The significance for the near-surface waters in the present case is less clear. Increased kinetic energy has also been observed near the shelf break. This has alternately been explained by reflection (Kroll and Niiler, 1976) and refraction (Rhines, 1971). In either event, a fraction of the impinging energy is transmitted onto the shelf and appears to be a significant influence in mixing across the shelf/slope boundary (Ou, 1980; Ou and Beardsley, 1980).

3. DATA SOURCES

3.1 Eulerian Current Data

At the outset of the study, a review of the history of moored current meter studies in the slope water region was performed to identify existing data sources. From a total inventory of more than 700 months of current meter data potentially available, roughly half of the records were selected for further analysis based on the criteria of accuracy and continuity. Data records collected prior to 1968 were automatically excluded in consideration of the uncertain accuracy associated with the instrumentation in use at that time.

After completion of the initial qualification process, the data base totaled over 150 separate records extending over roughly 300 current meter months within the period from 1968 to 1981. With such a large volume of data, often at high sampling rates, it was imperative to develop procedures to reduce the data base to more manageable proportions. This data reduction was achieved in two ways. First, stations which were in nearby locations in space (latitude, longitude, and depth) and time (i.e., not separated by too large a time gap) were concatenated into a single data set, thereby reducing the data base to a total of 77 continuous records.

Second, advection of disposed waste is relatively unaffected by high-frequency motions. Thus, it was permissible to low-pass filter the data without sacrificing essential information. The popular PL33 filter (Flagg, 1977) was used for this purpose. This filter has a half-power cut-off at 33 hours and is widely used to filter oceanographic data. After filtering, the data were subsampled at six-hour intervals, thus reducing the total number of points associated with each record. The data thus concatenated, filtered, and subsampled were archived on the EG&G database system maintained in Waltham, Massachusetts. Consecutive "station numbers" were assigned to each continuous data set in the order that it was archived. These station numbers were intended specifically for the purposes of the present study to facilitate identification and referencing of the individual data sets. In addition, a unique six-digit code was assigned to each data set as a routine procedure associated with the EG&G archiving system. This code is referred to as the Data Set Name or DSN.*

Figures 1a and 1b summarize the time intervals covered by individual data sets within the period from 1968 to 1976. The data sets are arranged in order by depth, beginning with the near-surface data. Figure 1c provides similar information for data sets within the period from 1979 to 1981. Figure 2 presents the geographic location of the moorings identified by station numbers and provides a general bathymetric view of the slope water region surrounding DWD 106.

---

*Refer to Table 3 for a complete summary of data set characteristics including a cross-indexing of station numbers and DSNs.

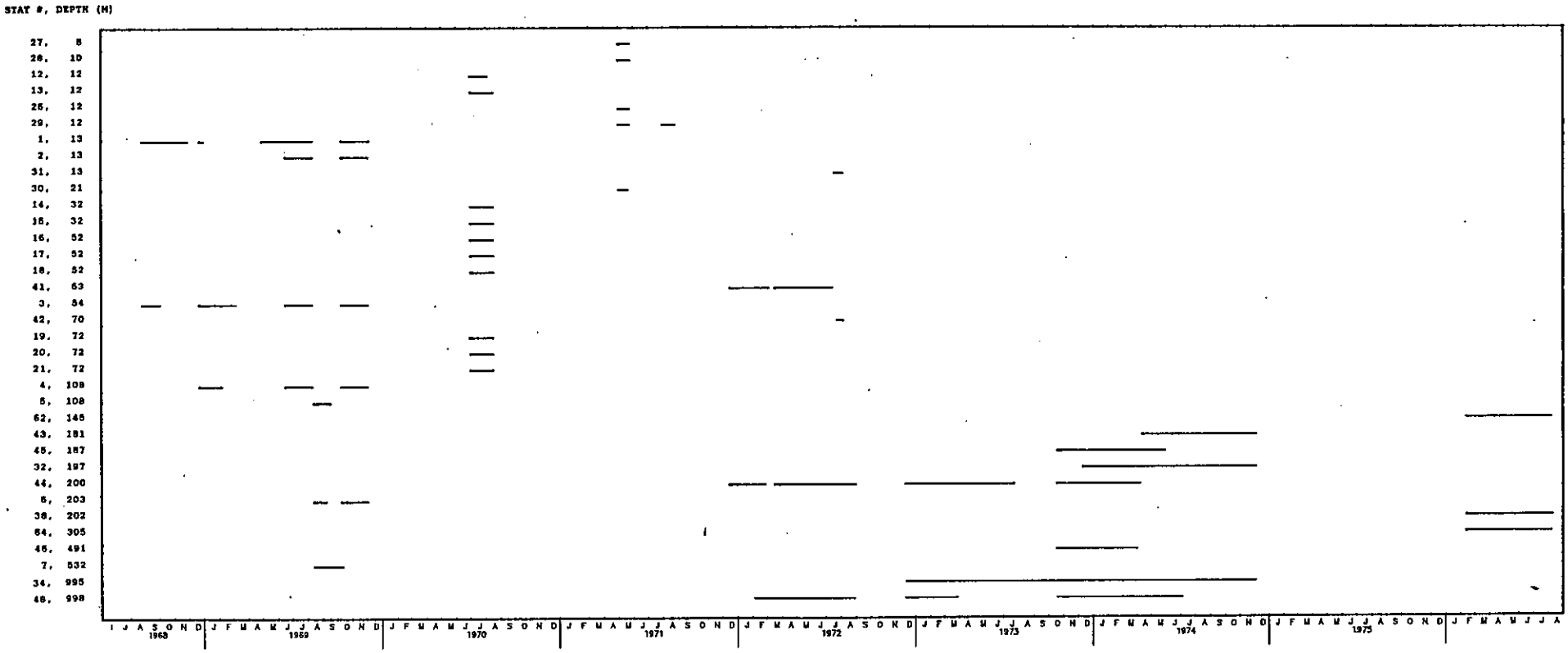

Figure 1a.

Coverage of current meter data from 1968 to 1976 above 1000-meter depth.

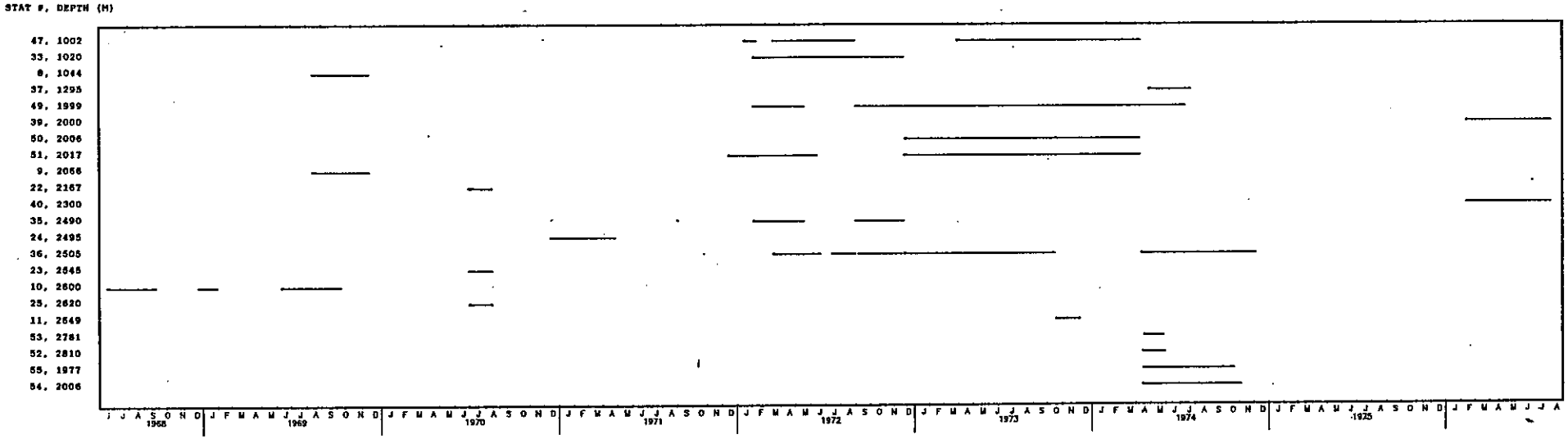

Figure 1b.

Coverage of current meter data from 1968 to 1976 below 1000-meter depth.

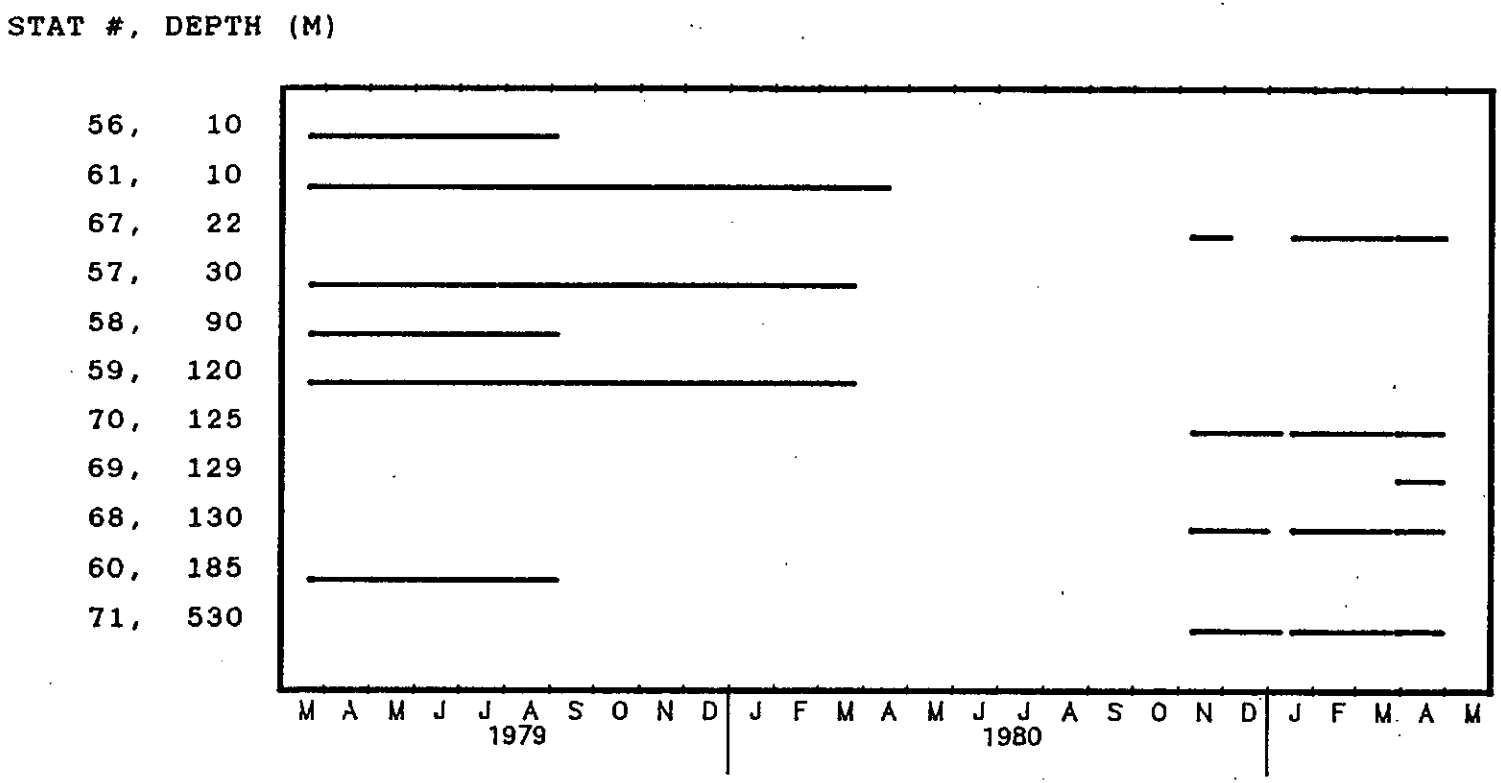

Figure 1c. Coverage of current meter data from 1979 to 1981.

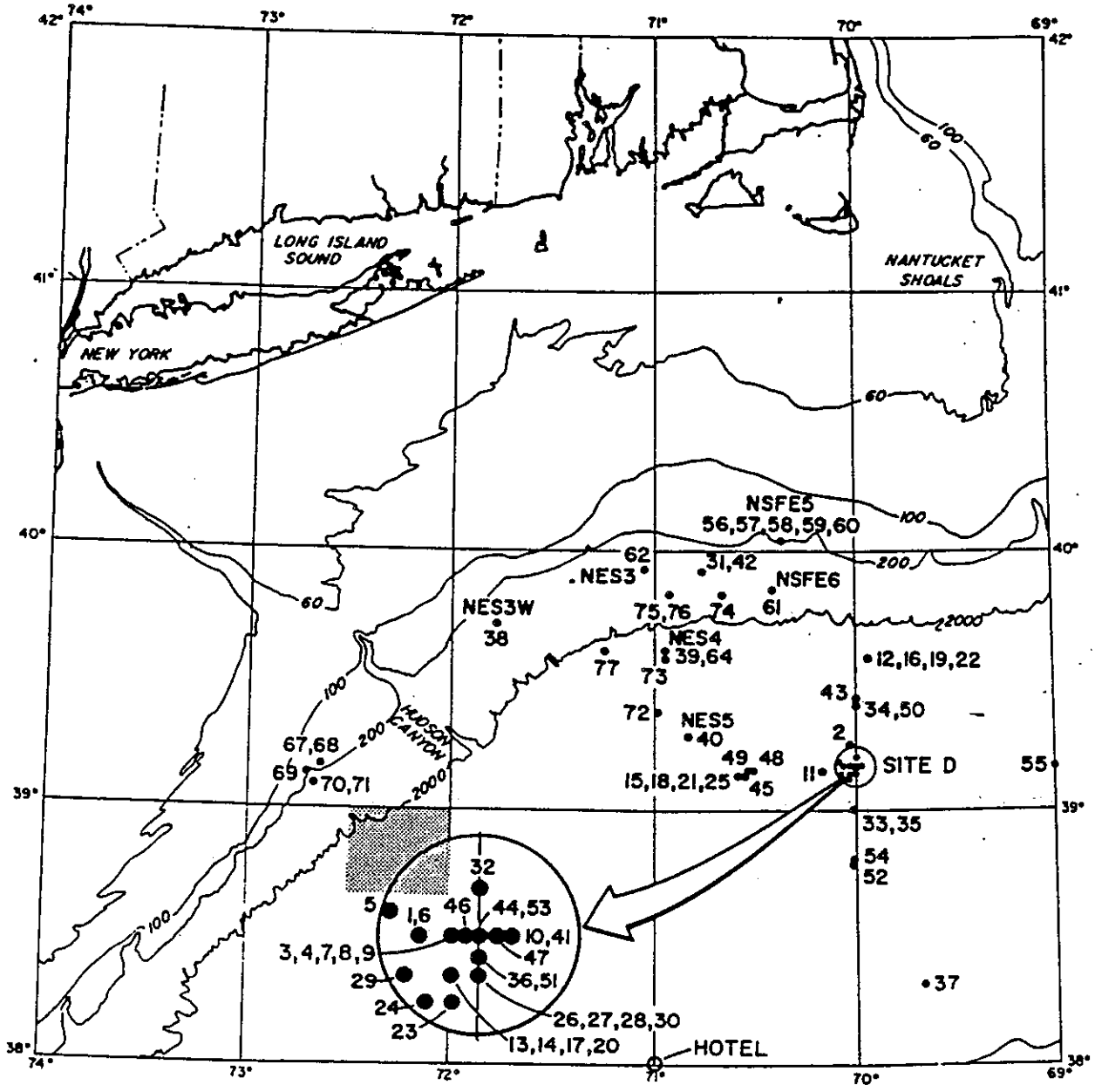

Figure 2. Location of wind and current stations in the slope water region. The shaded area indicates the boundaries of DWD 106. Wind data are available from Station Hotel and Site D.

The following sections describe the sources of the data and list the respective station numbers associated with each source.

3.1.1 Site D

The majority of the current meter data comes from Site D, which is a designation given by scientists at the Woods Hole Oceanographic Institution (WHOI) to a small area centered at 39°10'N and 70°00'W off the New England shelf. This site was extensively used between 1965 and 1974 to test instrument and mooring designs (Tarbell et al., 1980). We have included all of the data available at this site starting in 1968.

Station Nos: 1-11/13/14/17/20/23/24/26-30/32/36/41/43-47/51

3.1.2 Slope Arrays

From 1970 through 1974, concurrent with the moorings at Site D, there were several moorings deployed closer to the shelf break to study the dynamics of internal waves (Tarbell et al., 1980).

Station Nos: 12/15/16/18/19/21/22/25/31/33-35/42/48-50/72-77

3.1.3 The Rise Array

In 1974, eight moorings resulting in 21 instrument months of data were deployed along two transects beginning in the vicinity of Site D and extending south across the continental rise (Luyten, 1977).

Station Nos: 37/52-55

3.1.4 New York Bight

Five moorings crossing the shelf and extending onto the slope were deployed offshore of the New York Bight by WHOI in 1976. A total of 41 instrument months of data were collected (Tarbell et al., 1980).

Station Nos: 38-40/62/64

3.1.5 Nantucket Shoals Flux Experiment

A line of moorings crossing the shelf and extending onto the upper slope were deployed south of Nantucket in 1979 and 1980 by investigators from the National Marine Fisheries Service (NMFS), the United States Geological Survey (USGS) and Woods Hole Oceanographic Institution (WHOI) (R. Beardsley, private communication).

Station Nos: 56-61

3.1.6 Tom's Canyon Data

Seven current meter months of data from the slope region near Tom's Canyon (just inshore of DWD 106) were collected by EG&G in 1981 (EG&G, 1981).

Station Nos: 67-71

Additional data have been collected at locations along the Scotian Shelf/Slope (Smith and Petrie, 1982) by researchers from the Bedford Institute. The results obtained from this area are significant in the context of an overall understanding of slope water processes; however, it was considered unlikely that such current statistics would be transferable to the slope water region of interest in the vicinity of DWD 106. Recent current meter measurements from moorings in Lydonia and Baltimore Canyons were also considered for use in the data base, but the records were not immediately available.

3.2 Wind Data

Unfortunately, there are comparatively few continuous records of wind data available concurrent with the near-surface current meter data. Only two sources of data could be identified, the Woods Hole Buoy Group and the National Data Buoy Office (NDBO). The temporal coverage of the data sets is shown in Figure 3, and the geographic locations of the stations are included in Figure 2. The WHOI wind data records were collected at Site D in connection with various current meter deployments (Tarbell et al., 1980). The NDBO data comes from station Hotel, a weather station maintained by NOAA at 38°00'N and 71°00'W. These data were obtained from the National Climatic Center in Asheville, North Carolina. Processing of the wind data was similar to the processing of the current meter data. The data were low-pass filtered, decimated to six-hour intervals, and archived.

3.3 Lagrangian Current Data

Satellite-tracked drifting buoys give some of the best indications of long-term advective patterns. Although there is an extensive Lagrangian data base for the general area of the western North Atlantic, the number of surface drifter tracks within the slope water region is quite limited. We have been able to identify the following three sources:

1) EG&G, 1980. Tracks of three drifters deployed on Georges Bank which were drawn into the slope water region during the passage of separate warm core rings. The drifters were then quickly entrained in the Gulf Stream at points southeast of Georges Bank and carried eastward.

2) Bisagni, 1981. Tracks of two drifters deployed at DWD 106 and tracked for a total of four months. Both were carried southwestward, parallel to the shelf break, for roughly one month and then entrained in the Gulf Stream east of Cape Hatteras. This report also includes a description of three drifter releases performed by Raytheon Environmental Systems Center (unpublished data). These tracks extend from the deployment points south of Nantucket Shoals to Cape Hatteras and also lie roughly parallel to the shelf break.

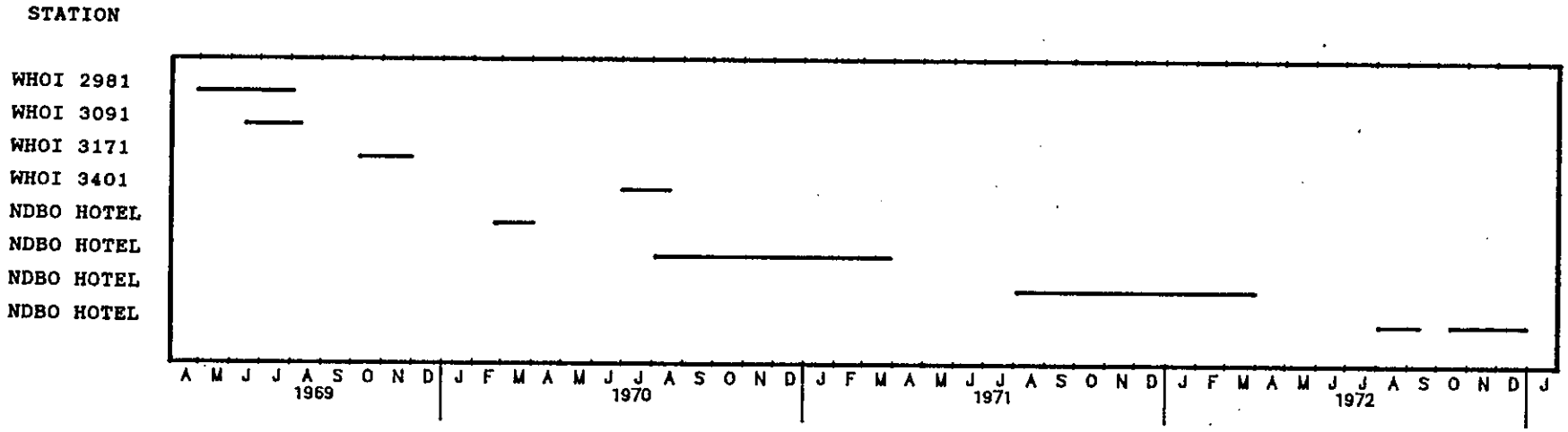

Figure 3. Coverage of wind data from 1969 to 1973.

3) Richardson, 1981. Tracks of multiple drifters deployed throughout the general area of the Gulf Stream system. One drifter in particular was deployed in the vicinity of DWD 106. It also exhibited a southwestwardly drift within the slope water region, followed by entrainment within the Gulf Stream east of Cape Hatteras.

It must be recognized that these drifter tracks are not precise indicators of water parcel trajectories and that the limited number of tracks does not provide an adequate statistical sample upon which to base quantitative conclusions. However, the data do generally provide important qualitative insight into the nature of the circulation and give us confidence in extending the results of current meter measurements into areas where no direct measurements have been made.

3.4 Data Quality and Validity

There are several basic questions concerning data quality and validity that must be addressed before interpreting the *in situ* current meter data. A primary concern is the extent of contamination in the records from extraneous, high-frequency wave and mooring-line motion. This concern is directed specifically at the early WHOI data which were obtained using EG&G Model 850 current meters deployed on surface moorings. All of the Site D near-surface data and much of the other near-surface data were collected this way. The Model 850 is a Savonius rotor instrument which records an average speed and instantaneous direction every five seconds and vector averages the result. After 1971, WHOI began using subsurface moorings exclusively and limited their data collection to regions below 200 meters. EG&G Vector Averaging Current Meters (VACMs) were gradually phased in at this point.

A comparison of current velocity spectra from VACMs and 850s deployed on surface moorings at depths of 8 to 21 meters at Site D is shown in Figure 4. These spectra reveal the high-frequency noise which is added to the 850 records due to wave and mooring line motion and aliased into lower frequencies. By processing these data with PL33, a low-pass filter designed to remove most of the energy in the records at periods less than 33 hours, the wave and mooring line contamination from the records is effectively removed. While the VACM is not ideally suited to use in the wave zone or with surface moorings, it has been used in this way on numerous recent research studies with considerable success and does appear to provide generally high-quality data. Table 1 shows the results of our processing of data from near-surface VACMs and 850s. As can be seen, the average speed, vector speed, vector direction, and maximum speed all appear quite similar with the small differences explained by the depth of the sensors.

Monthly mean speeds from current meters at Site D were examined as a function of depth and instrument/mooring type. These statistics indicate a relatively small instrumental bias in the surface-moored data toward higher monthly mean speeds using 850s at depth on the order of 2 to 3 cm/sec, which, while significant at 1000 meters and below, is not too disturbing in terms of the near-surface layers since typical speeds there are in a range near 20 cm/sec.

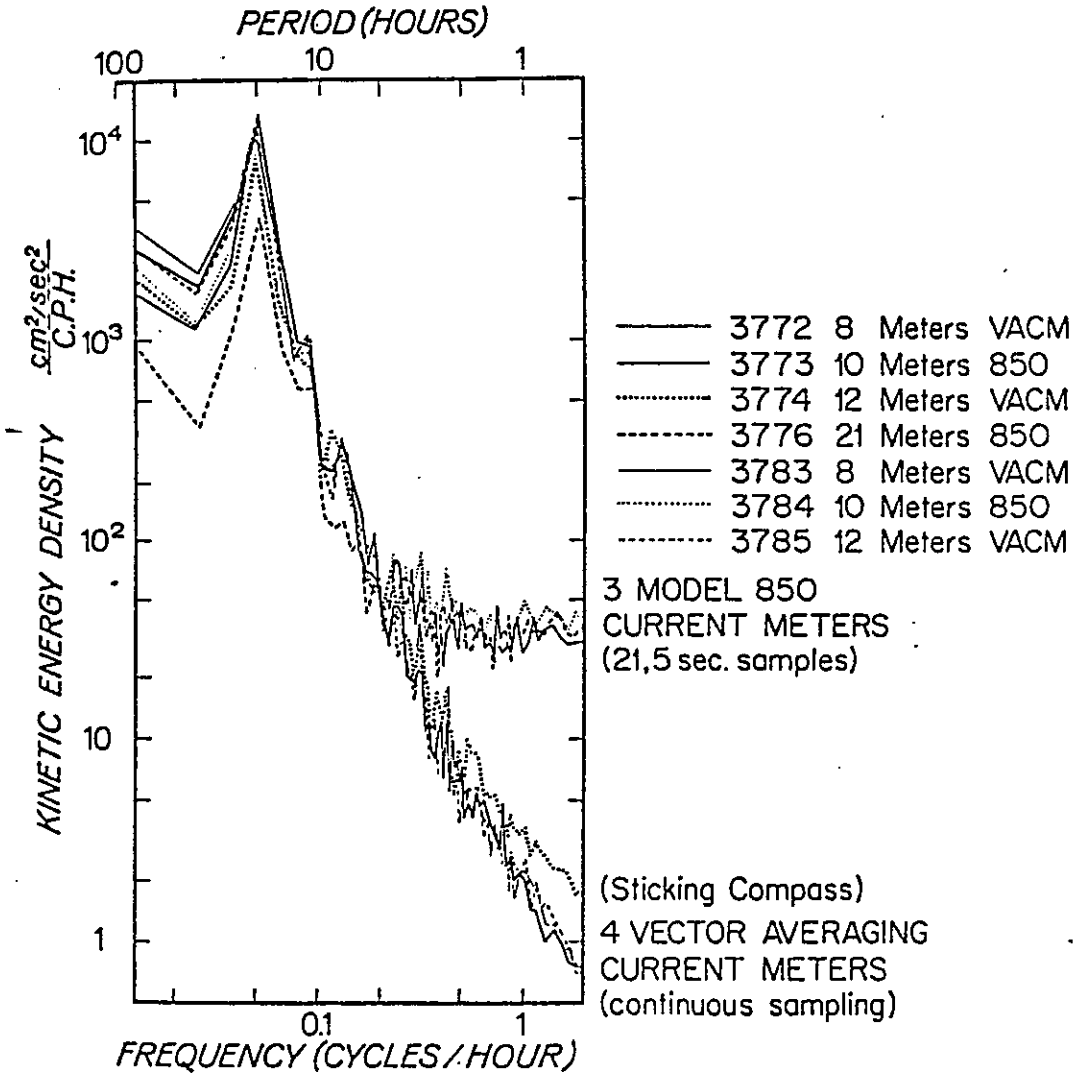

Figure 4. Comparison of current energy spectra from surface moorings at Site D (after Tarbell and Whitlatch, 1977).

Table 1. Statistics of near-surface currents measured from a surface mooring at Site D.

Depth (m)	Station No.	Instrument Type	Record Length (days)	Average Speed (cm/sec)	Vector Speed (cm/sec)	Vector Direction (^{o}True)	Maximum Speed (cm/sec)
Mooring 377							
8	27	VACM	23.8	18.9	13.9	262^{o}	40.6
10	28	850	25.0	17.6	14.2	258^{o}	39.1
12	29	VACM	23.6	—	13.0	270^{o}	—
21	30	850	20.8	15.4	12.8	264^{o}	36.8

Thus, mooring line motion, which is to a first approximation independent of depth on a mooring with a single surface buoy for flotation, impacted near-surface measurements from the 850s by an amount equivalent to a few cm/sec and tended to increase the measured mean. Similarly, the wave particle motions in the very-near surface (less than 50 meters depth) had an impact on measured speeds, but most of this contamination was removed in the filtering process. The conclusion, then, is that the data as presented are useful in terms of establishing long-term means to within a few cm/sec with the magnitude of the errors somewhat dependent on the wave climate. Errors of this size are unlikely to impact the results relative to questions concerning the suitability of DWD 106 as a disposal site.

A second major concern is whether data available from Site D and other widely dispersed locations in the slope region are applicable to DWD 106 in terms of the general circulation pattern. This has been investigated within the present study by computing coherences among various stations. In general, currents measured within 50 km in the along-slope direction and 20 km in the cross-slope direction appear to be reasonably coherent. As the distance between stations is increased beyond these limits, however, coherence between records drops to very low values and no strong direct relationship is apparent. Since the position of DWD 106 with respect to Site D is about 200 km downcoast and 50 km toward the shelf break, there is no reason to expect strong coherence between current records at these two locations. From a statistical viewpoint, however, there does appear to be a reasonable similarity between the sites, and it is these statistics which are principally relied upon in terms of evaluating DWD 106 as a waste disposal region. It is also apparent from the data that the coherence between records of finite length is destroyed by events such as eddies and other large-scale inhomogeneities known to be present in the slope region. Thus, while current measurements made upcoast of DWD 106 may not be particularly related on a real-time basis with those at DWD 106, there is little doubt that the long-term statistics are quite similar.

A final important question concerns the relationship of near-surface measurements and measurements from 200 meters depth. The importance of this question is that a 10-year data base is available at 200 meters depth, while only three years of data are available in the upper 100 meters. Coherence analyses were also performed between vertically separated pairs of current meters to determine the equivalence of current records over several depth ranges. Currents at 50 meters were significantly coherent with currents at 100 and 200 meters for periods greater than about four days. Coherence estimates in the low-frequency range varied from about 0.7 to 0.9. Coherence was lower for greater vertical separations and was also lower during winter than in summer at one station where seasonal data coverage was available. Instruments separated by the permanent thermocline were not significantly coherent at any frequency. This indicates that 200-meter data can be used to characterize the low-frequency variability of currents at shallower depths, except possibly during summer when the seasonal thermocline acts as a dynamic barrier between the surface and lower layers.

4. ANALYSIS OF CURRENT TIME SERIES

The previous sections have described the rationale for choosing the data used in this study. Interest is focused on the upper 200 meters of the slope water, but because of the small amount of data in this depth range for total water depths from 1500 to 2500 meters (the depth range at DWD 106), data from deeper water farther offshore are included in this analysis to increase spatial and temporal coverage. Table 2 presents the distribution of the collected data according to water and instrument depth. A total of 13,512.2 days of current data are available for analyses, but, as the table shows, only about 10% of the total available data comes from depths equivalent to those found at DWD 106. The data principally come from two types of measurement programs: those concerned with the continental shelf and shelf-edge processes and those concerned with low-frequency motions on the slope in the vicinity of the Gulf Stream. These measurement areas are, unfortunately, closer inshore or farther offshore than the area of DWD 106. The preponderance of the data comes from an investigation of slope water centered at Site D (~2700 m depth). The distribution of the data, according to instrument depth without regard to location, shows about 40% of the data collected above 200 meters and another 40% from below 1000 meters. The shallow data come primarily from the shelf-edge programs and the early measurements at Site D.

4.1 Statistical Summary

All of the data were low-pass filtered with a half-power cutoff at 33 hours and subsampled at six-hour intervals. Data sets from the same location and depth were concatenated. A statistical summary of this data is presented in Table 3. The station numbering used is special to this analysis and approximately chronological. The original data designation is included for possible reference. In addition, the EG&G data set name is included in the event that a reader wishes to obtain copies of the data for further analysis.

Warm core rings that are spawned by Gulf Stream meanders may, at times, dominate the current structure at a particular location along the slope, and must be considered in the analysis of the data. The occurrence and dynamics of the warm rings have been investigated by Halliwell and Mooers (1979), Smith (1978), Saunders (1971), Bisagni (1976), Lai and Richardson (1977), and Morgan and Bishop (1977). A multi-institutional study is presently underway to obtain a more complete understanding of warm ring kinematics and dynamics (Kester, 1981). Generally, the warm rings have diameters of order 100 km, extend downward 1000 to 1500 meters from the surface, and have maximum near-surface velocities of order 100 cm/sec. The rings are large anticyclonic meanders from the Gulf Stream which have separated and moved northward and usually westward. Rings are commonly formed south of Georges Bank and Nova Scotia and propagate westward at speeds of 5 to 10 cm/sec.

Because of the large currents within the rings, they can statistically dominate a current record, obscuring information about the background current field. Since the goal of this study is to describe the background field, a method is needed to separate the two signals. Temperature and current magnitude are the two main signatures for the rings, and some criteria based on these would be the most effective. However, temperature was not recorded on

Table 2. Distribution of current data by water depth and instrument depth.

Current Data Coverage

Water Depth (m)	Record days	Percentage
100–500	2,069.5	15.3
500–1000	788.2	5.8
1000–1500	–	0
1500–2000	–	0
2000–2500	1,328.2	9.8
2500–3000	8,990.1	66.5
>3000	336.2	2.4
Total	13,512.2	100.0

Instrument Depth (m)	Record days	Percentage
0–50	1,781.1	13.2
50–200	3,613.7	26.7
200–500	606.1	4.6
500–1000	1,708.0	12.6
1000–2000	2,448.9	18.1
>2000	3,354.4	24.8
Total	13,512.2	100.0

Table 3.

Statistical summary of current data.

Station No.	Dates	Location	Original Designation	Instrument Depth (meters)	Water Depth	Total Days of Data	Average Speed (cm/sec)	Speed Standard Deviation (cm/sec)	Maximum Speed (cm/sec)	Mean East (cm/sec)	East Standard Deviation (cm/sec)	Mean North (cm/sec)	North Standard Deviation (cm/sec)	Vector Averaged Speed (cm/sec)	Vector Averaged Direction (°True)	Statistics with Eddies Removed							Data Set Name	Mooring Type
																No. of Eddy-Free Days of Data	Mean East (cm/sec)	East Standard Deviation (cm/sec)	Mean North (cm/sec)	North Standard Deviation (cm/sec)	Vector Averaged Speed (cm/sec)	Vector Averaged Direction (°True)		
1	8/24/68-12/7/69	39°10'N 70°03'W	2742,2803,2842, 2983,3173	13	2685	268.5	28.5	18.1	115.1	-6.3	18.3	3.4	27.5	7.2	298°	179.2	-10.0	12.9	4.9	15.0	11.1	296°	407327	S/850
2	6/15/69-12/4/69	39°10'N 70°02'W	3093,3181	13	2678	112.0	38.5	21.5	81.9	6.8	25.8	8.4	34.1	10.8	39°	65.2	-5.9	18.2	10.3	14.6	11.9	330°	407328	S/850
3	8/24/68-12/4/68	39°10'N 70°02'W	2743,2843,3095, 3174	54	2685	226.2	22.1	15.4	74.5	-4.4	15.8	-0.4	21.4	4.4	265°	181.2	-8.0	11.3	1.1	11.8	8.1	276°	407329	S/850
4	12/2/68-12/3/69	39°10'N 70°02'W	2845,3096,3175	108	2690	159.0	22.7	15.9	67.1	-4.2	16.1	-4.1	21.8	5.9	226°	114.0	-6.9	12.8	-2.0	10.8	7.2	254°	407330	S/850
5	8/13/69-9/17/69	39°11'N 70°05'W	3116	108	2685	34.5	10.7	7.2	28.6	0.4	8.0	-4.1	9.3	4.1	174°								407331	S/850
6	8/13/69-12/13/69	39°10'N 70°03'W	3101,3176	203	2680	81.8	20.9	16.0	54.4	-0.2	13.8	-4.2	22.0	4.2	183°	39.8	-3.9	7.3	0.2	6.9	3.9	273°	407332	S,I/850
7	8/13/69-10/12/69	39°10'N 70°02'W	3102	532	2683	59.2	6.2	3.3	15.2	-1.3	6.0	-2.0	2.9	2.4	213°								407333	I/850
8	8/13/69-12/6/69	39°10'N 70°02'W	3103	1044	2683	114.8	6.2	3.8	20.6	-2.5	4.8	-2.4	4.1	3.5	226°								407334	I/850
9	8/13/69-12/8/69	39°10'N 70°01'W	3104	2066	2683	116.2	4.1	2.2	10.6	-1.6	3.4	-0.4	2.7	1.6	256°								407335	I/850
10	6/17/68-10/11/69	39°10'N 69°58'W	2681,2871,3021	2600	2685	262.0	5.8	3.7	23.5	-2.1	3.9	0.4	5.2	2.1	281°								407336	I/850
11	10/18/73-12/7/73	39°09'N 70°10'W	5081	2649	2714	49.0	4.9	2.7	12.6	-1.9	4.0	-0.3	3.5	1.9	261°								407337	I/VACM
12	6/29/70-8/4/70	39°35'N 69°56'W	3383	12	2322	35.8	21.5	7.2	43.6	3.1	7.6	19.6	7.9	19.8	9°	2.8	7.2	8.7	5.1	6.7	8.8	54°	407338	S/850
13	6/29/70-8/17/70	39°08'N 70°02'W	3393	12	2682	48.2	11.0	6.0	31.4	-5.7	7.7	-2.1	7.8	6.1	250°								407339	S/850
14	6/29/70-8/17/70	39°08'N 70°02'W	3394	32	2682	48.2	11.7	6.4	28.9	-9.4	7.5	0.6	5.8	9.4	274°								407340	S/850
15	6/30/70-8/18/70	39°08'N 70°35'W	3403	32	2754	48.2	9.2	6.3	27.2	-3.5	7.6	-4.7	5.7	5.9	217°								407341	S/850
16	6/29/70-8/17/70	39°35'N 69°56'W	3385	52	2322	48.2	9.5	3.9	23.0	-0.9	4.2	7.9	5.0	8.0	354°								407342	S/850
17	6/29/70-8/17/70	39°08'N 70°02'W	3395	52	2682	48.2	10.9	5.8	25.3	-8.4	6.9	-2.3	5.4	8.7	255°								407343	S/850
18	6/30/70-8/18/70	39°08'N 70°35'W	3404	52	2754	48.2	10.4	6.2	26.5	-6.1	8.4	-2.5	5.8	6.6	248°								407344	S/850
19	6/29/70-8/17/70	39°35'N 69°56'W	3386	72	2322	48.2	8.5	3.9	26.5	-0.6	4.6	5.7	5.7	5.7	354°								407344	S/850
20	6/29/70-8/17/70	39°08'N 70°02'W	3396	72	2682	48.2	11.8	6.0	27.5	-9.4	7.3	-1.4	5.5	9.5	262°								407346	S/850
21	6/30/70-8/18/70	39°08'N 70°35'W	3406	72	2754	48.2	11.0	7.0	32.8	-6.5	9.5	-3.1	5.4	7.2	244°								407347	S/850
22	6/29/70-8/17/70	39°35'N 69°56'W	3387	2167	2322	48.2	5.6	2.5	11.5	-4.0	4.0	0.4	2.4	4.0	276°								407348	S/850
23	6/29/70-8/18/70	39°07'N 70°02'W	3397	2545	2682	48.2	6.1	3.4	15.0	-2.1	2.6	-0.8	6.1	2.2	249°								407349	S/850
24	12/13/70-4/27/71	39°07'N 70°03'W	3585	2495	2680	134.0	4.3	2.7	14.4	-2.0	3.5	-0.7	2.9	2.1	251°								407350	I/850
25	6/30/70-8/18/70	39°08'N 70°35'W	3407	2620	2754	48.2	6.1	2.2	12.6	-0.7	5.3	-1.3	3.5	1.5	208°								407351	S/850

Table 3. (con't)

Statistical summary of current data.

Station No.	Dates	Location	Original Designation	Instrument Depth (meters)	Water Depth	Total Days of Data	Average Speed (cm/sec)	Speed Standard Deviation (cm/sec)	Maximum Speed (cm/sec)	Mean East (cm/sec)	East Standard Deviation (cm/sec)	Mean North (cm/sec)	North Standard Deviation (cm/sec)	Vector Averaged Speed (cm/sec)	Vector Averaged Direction (°True)	Statistics with Eddies Removed							Data Set Name	Mooring Type
																No. of Eddy-Free Days of Data	Mean East (cm/sec)	East Standard Deviation (cm/sec)	Mean North (cm/sec)	North Standard Deviation (cm/sec)	Vector Averaged Speed (cm/sec)	Vector Averaged Direction (°True)		
26	4/29/71-5/24/71	39°08'N 70°00'W	3785	12	2665	23.8	19.4	11.7	43.5	-15.7	13.1	-2.5	9.4	15.9	261°								407352	S/VACM
27	4/29/71-5/24/71	39°08'N 70°00'W	3772	8	2665	23.8	18.9	10.3	40.6	-13.8	12.8	-1.8	10.3	13.9	262°								407353	S/VACM
28	4/29/71-5/24/71	39°08'N 70°00'W	3773	10	2665	25.0	17.6	10.7	39.1	-13.9	11.9	-3.0	9.1	14.2	258°								407354	S/850
29	4/29/71-8/26/71	39°08'N 70°04'W	3774,3963	12	2665	50.8	22.2	17.7	95.2	-7.8	10.0	14.1	21.1	16.1	331°	30.8	-10.5	11.4	3.9	18.8	11.2	290°	407355	S/VACM,850
30	4/29/71-5/21/71	39°08'N 70°00'W	3776	21	2665	20.8	15.4	10.5	36.8	-12.7	11.5	-1.4	7.3	12.8	264°								407356	S/850
31	7/17/72-8/4/72	39°55'N 70°46'W	4623	13	501	18.2	6.0	2.4	13.6	-1.1	4.6	0.3	4.5	1.1	285°								407358	I/VACM
32	12/9/73-12/5/74	39°12'N 70°00'W	5172,5173	197	2647	360.2	21.8	14.5	54.9	-6.3	12.6	-0.4	22.1	6.3	266°	199.5	-4.5	9.7	-0.8	10.0	4.6	260°	407360	I/VACM
33	2/3/72-12/10/72	39°00'N 70°01'W	4221,4491,4651	1020	2724	307.0	5.7	3.5	16.6	-4.2	3.9	-1.3	3.1	4.4	253°								407367	I/850
34	12/12/72-12/5/74	39°24'N 70°00'W	4791,4901,5062, 5232	995	2558	718.0	5.7	3.9	29.1	-3.0	5.1	-1.1	3.4	3.2	250°	698.0	-3.1	4.7	-0.8	3.0	3.2	255°	407368	I/850,VACM
35	2/3/72-12/10/72	39°00'W 70°01'W	4222,4652	2490	2724	204.8	5.6	3.4	19.4	-3.3	4.2	-1.4	3.6	3.6	247°								407371	I/850
36	3/15/72-12/5/74	39°09'N 70°00'W	4297,4683,4775, 4914,5247	2505	2656	780.5	6.2	3.1	18.1	-2.4	4.2	-0.9	4.9	2.6	249°								407372	S,I/850,VACM
37	4/27/74-7/23/74	38°19'N 69°39'W	5411	1295	3583	85.5	7.8	5.3	20.2	-1.0	9.0	0.2	2.5	1.0	281°								407373	I/VACM
38	2/12/76-8/10/76	39°43'N 71°47'W	5901	302	500	180.0	6.6	4.3	23.8	0.7	6.1	1.1	4.7	1.3	32°	109.8	-0.6	4.7	-0.4	4.4	0.7	236°	407376	I/VACM
39	2/12/76-8/7/76	39°37'N 70°57'W	5882	2000	2305	177.5	5.3	3.3	16.4	-3.4	5.0	-0.3	1.7	3.4	265°								407377	I/VACM
40	2/12/76-8/7/76	39°17'N 70°50'W	5891	2000	2645	177.0	3.4	1.9	11.2	-1.8	3.0	-0.1	1.8	1.8	267°								407378	I/VACM
41	12/14/71-7/15/72	39°10'N 69°58'W	4203,4293	53	2654	200.8	17.0	11.6	58.2	-8.8	13.1	-1.3	13.2	8.9	262°	163.0	-5.0	8.9	-1.8	10.3	5.3	250°	407357	S/850
42	7/17/72-8/5/72	39°55'N 70°46'W	4624	70	501	18.3	6.1	2.5	13.7	0.5	4.7	1.0	4.6	1.1	26°								407359	I/VACM
43	4/11/74-12/6/74	39°26'N 70°00'W	5231,5241	181	2504	237.3	21.0	16.6	71.4	-5.0	16.6	0.1	20.4	5.0	271°	182.5	-6.1	10.8	-2.8	10.4	6.7	245°	407361	I/VACM
44	12/14/71-4/9/74	39°10'N 70°00'W	4204,4294,4772, 4911,5061	200	2654	640.3	19.9	16.1	70.5	-5.6	12.0	-4.0	21.5	6.9	234°	417.2	-6.5	5.9	-2.2	8.2	6.8	251°	407362	S,I/850
45	10/18/73-5/30/74	39°08'N 70°33'W	5091,5251	187	2746	223.0	26.1	20.8	89.7	-17.0	20.1	-2.3	20.4	17.2	262°	136.2	-5.4	8.1	-1.5	10.8	5.6	254°	407363	I/850,VACM
46	10/16/73-4/3/74	39°10'N 70°01'W	5072	491	2662	166.8	8.6	4.9	18.9	-2.8	6.2	0.5	7.1	2.8	280°	91.2	-1.6	6.5	-0.7	3.6	1.7	246°	407364	I/850
47	1/15/72-4/11/74	39°10'N 69°59'W	3954,4205,4295, 4912,5073	1002	2428	570.8	5.8	3.1	20.0	-3.0	4.3	-1.5	3.8	3.4	243°	547.8	-3.1	4.2	-1.4	3.3	3.4	245°	407365	S,I/850
48	2/3/72-7/6/74	39°09'N 70°31'W	4231,4501,4781, 5092,5252	998	2729	572.3	4.7	3.1	16.8	-2.8	4.0	-0.6	2.8	2.9	258°								407366	I/850,VACM
49	2/3/72-7/13/74	39°09'N 70°32'W	4232,4502,4662, 4782,4922,5093,5253	1999	2729	780.3	4.9	3.0	21.3	-2.0	4.5	-0.4	2.9	2.0	259°								407369	I/850,VACM
50	12/12/72-4/10/74	39°24'N 70°00'W	4792,4902,5063, 5233	2006	2558	477.8	4.4	2.9	22.1	-1.3	4.3	-0.3	2.6	1.3	257°								407370	I/850,VACM
51	12/14/71-4/11/74	39°09'N 70°00'W	4206,4296,4774, 4913,5074	2017	2654	677.0	5.3	3.0	19.3	-2.9	4.0	-1.3	3.4	3.2	246°								407374	S,I/850

Table 3. (con't)

Statistical summary of current data.

Station No.	Dates	Location	Original Designation	Instrument Depth (meters)	Water Depth	Total Days of Data	Average Speed (cm/sec)	Speed Standard Deviation (cm/sec)	Maximum Speed (cm/sec)	Mean East (cm/sec)	East Standard Deviation (cm/sec)	Mean North (cm/sec)	North Standard Deviation (cm/sec)	Vector Averaged Speed (cm/sec)	Vector Averaged Direction (°True)	Statistics with Eddies Removed: No. of Eddy-Free Days of Data	Mean East (cm/sec)	East Standard Deviation (cm/sec)	Mean North (cm/sec)	North Standard Deviation (cm/sec)	Vector Averaged Speed (cm/sec)	Vector Averaged Direction (°True)	Data Set Name	Mooring Type
52	4/13/74-6/1/74	38°47'N 70°01'W	5262	2810	3007	46.5	10.3	6.3	25.7	-1.8	8.9	0.6	8.0	1.9	288°	32.5	-4.6	6.9	-3.4	4.5	5.8	233°	407375	I/VACM
53	4/7/74-5/28/74	39°10'N 70°00'W	5272	2781	2978	35.8	6.7	3.9	15.0	1.5	7.2	-0.5	2.6	1.6	108°								407379	I/VACM
54	4/13/74-11/5/74	38°47'N 70°01'W	5261	2006	3007	204.2	7.0	3.8	19.0	-3.8	5.9	-0.9	3.7	3.9	257°								407380	I/VACM
55	4/14/74-10/22/74	39°10'N 60°00'W	5271	1977	2978	190.0	6.0	3.1	14.7	-3.4	4.7	-1.6	2.9	3.8	245°								407488	I/VACM
56	3/20/79-9/3/79	40°02'N 70°22'W	NSFE51	10	198	168.0	13.3	7.4	38.5	1.0	12.5	1.0	8.6	1.4	45°	101.2	-4.6	10.4	-0.1	8.2	4.6	268°	407519	S/VACM
57	3/20/79-3/20/80	40°02'N 70°22'W	NSFE52	30	198	369.8	11.8	8.4	53.1	-2.7	12.0	-0.9	7.5	2.8	252°	257.2	-5.1	11.3	-2.1	8.0	5.5	248°	407520	I/VACM
58	3/20/79-9/9/79	40°02'N 70°22'W	NSFE53	90	198	168.0	9.2	5.1	26.8	3.9	8.1	2.2	5.1	4.5	60°	100.8	2.2	7.4	0.5	5.1	2.3	76°	407521	I/VACM
59	3/20/79-3/20/80	40°02'N 70°22'W	NSFE54	120	198	369.8	9.4	6.8	42.1	0.3	10.8	1.0	4.2	1.0	17°	257.2	-1.8	10.5	0.3	4.0	1.8	278°	407522	I/VACM
60	3/20/79-9/3/79	40°02'N 70°22'W	NSFE55	185	198	168.0	6.1	4.2	25.6	-0.8	6.7	-1.5	2.7	1.7	208°	100.8	-0.2	6.0	-1.9	2.3	1.9	186°	407523	I/VACM
61	3/20/79-4/16/80	39°51'N 70°25'W	NSFE61	10	810	393.2	16.9	9.7	54.3	3.6	15.9	-0.9	10.7	3.7	104°	279.5	-3.3	12.4	-2.4	10.8	4.1	233°	407524	S/VACM
62	2/11/76-8/7/76	39°56'N 71°3'W	5871	145	496	178.0	9.8	6.0	33.5	-0.2	9.4	1.5	6.4	1.5	354°	168.0	-1.2	8.4	1.1	6.4	1.6	312°	407525	I/VACM
64	2/11/76-8/7/76	39°37'N 70°57'W	5881	305	2305	177.5	7.0	4.5	22.8	-3.6	6.0	-0.7	4.4	3.7	359°								407527	I/VACM
67	11/6/80-4/30/81	39°10'N 72°38'W	Tom's Canyon	22	140	126.8	17.1	9.6	49.9	-5.3	11.8	-6.7	13.1	8.5	218°	111.8	-8.3	8.0	-9.6	10.5	12.7	221°	407758	I/CT-3
68	11/6/80 4/30/81	39°10'N 72°38'W	Tom's Canyon	130	140	151.3	12.4	8.0	38.5	-5.5	8.4	-3.7	10.3	6.6	236°	136.0	-6.9	7.1	-5.9	7.6	9.1	229°	407759	I/RCM
69	3/26/81-4/30/81	39°08'N 72°42'W	Tom's Canyon	129	140	31.3	10.1	7.3	33.8	-6.9	6.7	-3.6	7.1	7.8	242°								407760	I/RCM
70	11/7/80-4/30/81	39°01'N 72°41'W	Tom's Canyon	125	135	158.5	10.0	7.0	33.8	-4.3	7.4	-2.6	8.3	4.9	238°	143.8	-5.5	6.1	-4.3	6.1	7.0	232°	407761	I/RCM
71	11/7/80-4/30/81	39°01'N 72°41'W	Tom's Canyon	530	540	158.5	1.8	1.1	6.1	0.9	1.4	0.6	1.0	1.1	56°	143.8	1.0	1.5	0.5	1.1	1.1	27°	407762	I/RCM
72	8/20/70-10/5/70	39°23'N 70°59'W	3451	1504	2527	46				-2.8	3.1	0.3	1.7	2.8	276°									I/850
73	8/20/70-12/2/70	39°35'N 70°58'W	3461	2163	2263	111				-6.4	10.0	0.2	2.6	6.4	272°									I/850
74	8/20/70-12/2/70	39°50'N 70°40'W	3471	776	876	104				-6.4	6.3	1.6	1.5	6.6	284°									I/850
75	8/20/70-9/30/70	39°50'N 70°56'W	3491	846	943	45				-2.0	3.7	1.0	1.0	2.2	296°									I/850
76	8/20/70-10/9/70	39°50'N 70°56'W	3501	888	993	51				-4.6	5.8	1.8	1.3	4.9	291°									I/850
77	8/20/70-12/9/70	39°37'N 71°15'W	3511	2052	2150	111				-5.1	7.9	-0.4	2.2	5.1	266°									I/850

in situ instrumentation until the mid-1970s so that for most of the data sets only velocity can be used to distinguish warm rings. The velocity signature of warm rings varies considerably across the slope and rise and also with depth. In the vicinity of Site D, the canonical ring passes directly over the moorings which results in an easily identifiable northward current pulse, followed by a southward pulse. Farther north where the water depth restricts the onshore penetration of the rings, the passage of a warm ring produces a strong eastward or northeastward flow, sometimes with a clockwise turning of the current vector. This signature, especially if relatively weak, can easily be confused with wind-driven events. Lastly, for instrument depths greater than 1000 meters, it is very difficult to distinguish current fluctuations caused by rings. Where it is difficult to identify the passage of a ring from the background velocity signature, the current statistics will not be biased to a great extent by its inclusion.

All the current records were reviewed for the presence of rings using the current velocity as the primary discriminant. For those few records with temperature, this variable was also used to identify the passage of warm rings. Where the velocity data did not provide a clear indication of the presence of a ring, the Experimental Ocean Frontal Analysis charts from the Naval Hydrographic Office and Monthly Gulf Stream Summaries from NOAA were examined. Those periods judged to be contaminated by rings were removed to form ring-free records for analysis. A conservative approach was taken so that marginal data were removed. Thus, in Table 3, a second set of statistics is included for those records that were edited to remove warm ring contamination. This editing process reduced the total data set by 8%, and reduced by 22% those records shallower than 1000 meters.

The statistics of the low-frequency currents presented in Table 3 are graphically displayed in a series of figures showing the vertical and horizontal dependence of the parameters. Figure 5 shows the vertical distribution of the maximum observed low-frequency current speed for each station regardless of location. Since the maximum speed is a parameter dominated by special events such as the passage of rings or wind forcing, there was no attempt to separate those periods influenced by rings as is done elsewhere. There is a marked difference between the maximum speeds observed above 200 meters and those below. Above 200 meters, about 30% of the records had maximum speeds greater than 50 cm/sec with 115 cm/sec observed in one record from Site D. The remaining two-thirds of the records have maximum speeds falling between 25 and 40 cm/sec. Below 200 meters the maximum speeds are remarkably uniform in the vertical down to 3000 meters. With only a few exceptions, all the maximum speeds in this region are between 10 and 25 cm/sec.

In order to summarize the flow field over the slope, the currents were vertically and horizontally averaged. For the horizontal averaging, records from stations located along approximately the same isobath were combined into nine distinct regions. The numbering of these regions is independent of the station numbering scheme; in addition, data from Site D were kept separate from those of other regions. The results of the averaging are presented in Tables 4a and b and in Figures 6a and b. In Table 4a and Figure 6a, all the data are included while Table 4b and Figure 6b have had the influence of warm rings removed. In addition, Figure 6b shows the mean current vectors only for those locations with more than 100 days of data.

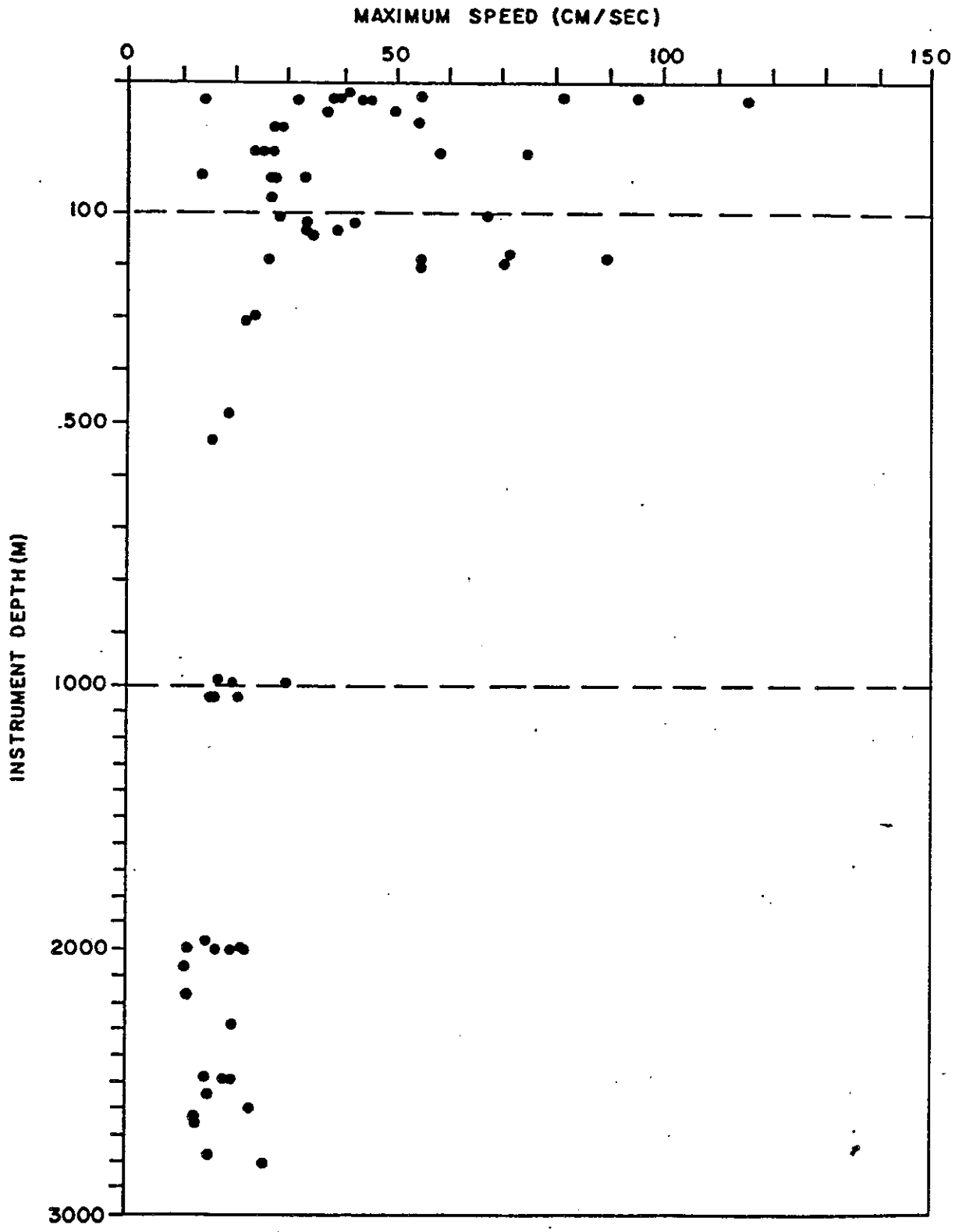

Figure 5. Vertical distribution of maximum observed low-frequency current speed in the slope region regardless of location. The results include the effect of warm rings. Note the scale changes for the depth axis.

Table 4a. Vertically averaged current statistics with warm rings included.

Area	Depth Range (m)	Data Length (days)	East Component Mean (cm/s)	East Component Std. Dev. (cm/s)	North Component Mean (cm/s)	North Component Std. Dev. (cm/s)	Vector Average Speed (cm/s)	Vector Average Dir. (°T)
Site D	0-55	984.3	-7.41	14.75	0.90	19.90	7.46	277
	70-110	241.7	-4.58	14.06	-2.39	18.39	5.17	242
	200	1082.3	-5.42	12.43	-2.82	21.79	6.11	242
	490-530	226.0	-2.41	6.17	-0.15	6.37	2.41	266
	1002-1044	685.6	-2.92	4.39	-1.65	3.86	3.35	240
	2017-2066	783.2	-2.71	3.94	-1.17	3.32	2.95	247
	2495-2781	1260.5	-2.17	4.18	-0.59	4.82	2.25	255
1	1020	307.0	-4.2	3.9	-1.3	3.1	4.2	253
	2006	204.2	-3.8	5.9	-0.9	3.7	3.9	257
	2490-2810	251.3	-3.0	5.4	-1.0	4.8	3.2	252
2	32-52	96.4	-4.8	8.1	-3.6	5.8	6.0	233
	72	48.2	-6.5	9.5	-3.1	5.4	7.2	244
	187	223.0	-17.0	20.1	-2.3	20.4	17.2	262
	998	572.3	-2.8	4.0	-0.6	2.8	2.9	258
	1999	780.3	-2.0	4.5	-0.4	2.9	2.0	259
	2620	48.2	-0.7	5.3	-1.3	3.5	1.5	208
3	181	237.3	-5.0	16.6	0.1	20.4	5.0	272
	995	718.0	-3.0	5.1	-1.1	3.4	3.2	249
	1295-1504	131.5	-1.6	7.5	0.2	2.2	1.6	277
	2006-2300	654.8	-1.4	4.0	-0.2	2.4	1.4	262
4	12-52	84.0	0.3	6.2	12.9	8.6	12.9	001
	72	48.2	-0.6	4.6	5.7	5.7	5.7	354
	305	177.5	-3.6	6.0	-0.7	4.4	3.7	259
	2000-2167	447.7	-4.6	7.3	-0.1	2.2	4.6	269
5	776-888	200.0	-5.0	5.9	1.5	1.4	5.2	287
6	10-13	411.4	3.4	15.6	1.0	4.6	1.1	026
	70	18.3	0.5	4.7	1.5	6.4	1.5	354
	145	178.0	-0.2	9.4	1.1	4.7	1.3	032
7	10-30	537.8	-1.5	12.3	-0.3	7.9	1.5	259
	90-120	537.8	1.4	10.2	1.4	4.5	2.0	045
	185	168.0	-0.8	6.7	-1.5	2.7	1.7	208
8	302	180.0	0.7	6.1	1.1	4.7	1.3	032
9	22	125.5	-5.4	11.8	-6.8	13.1	8.7	218
	129-130	182.3	-5.7	8.1	-3.7	9.7	6.8	237

Table 4b. Vertically averaged current statistics without warm rings.

Area	Depth Range (m)	Data Length (days)	East Component Mean (cm/s)	East Component Std. Dev. (cm/s)	North Component Mean (cm/s)	North Component Std. Dev. (cm/s)	Vector Average Speed (cm/s)	Vector Average Dir. (°T)
Site D	0–55	613.5	-8.2	10.4	1.2	11.1	8.6	274
	70–110	196.7	-6.2	11.4	-2.2	9.5	6.6	250
	200	656.5	-5.7	7.4	-1.6	8.8	5.9	254
	490–530	150.4	-1.5	6.3	-1.2	3.4	1.9	231
	1002–1044	662.6	-3.0	4.3	-1.6	3.5	3.4	242
	2017–2066	783.2	-2.7	3.9	-1.2	3.3	3.0	246
	2495–2781	1260.5	-2.2	4.2	-0.6	4.8	2.3	255
1	1020	307.0	-4.2	3.9	-1.3	3.1	4.4	253
	2006	204.2	-3.8	5.9	-0.9	3.7	3.9	257
	2490–2810	251.3	-3.0	5.4	-1.0	4.8	3.2	252
2	32–72	48.2*	-5.4	8.6	-3.4	5.7	6.4	238
	187	136.2	-5.4	8.1	-1.5	10.8	5.6	254
	998	572.3	-2.8	4.0	-0.6	2.8	2.9	258
	1999	780.3	-2.0	4.5	-0.4	2.9	2.0	259
	2620	48.2*	-0.7	5.3	-1.3	3.5	1.5	208
3	181	182.5	-6.1	10.8	-2.8	10.4	6.7	245
	995	698.0	-3.1	4.7	-0.8	3.0	3.2	256
	1295–1504	131.5	-1.6	7.5	0.2	2.2	1.6	277
	2006–2300	654.8	-1.4	4.0	-0.2	2.4	1.4	262
4	12–52	51.0*	-0.5	4.9	7.8	5.1	7.8	356
	72	48.2*	-0.6	4.6	5.7	5.7	5.7	354
	305	177.5	-3.6	6.0	-0.7	4.4	3.7	259
	2000–2167	447.7	-4.6	7.3	-0.1	2.2	4.6	269
5	776–888	200.0	-5.0	5.9	1.5	1.4	5.2	287
6	10–13	297.7	-3.2	12.1	-2.2	10.5	3.9	235
	70	18.3*	0.5	4.7	1.0	4.6	1.1	026
	145	168.0	-1.2	8.4	1.1	6.4	1.6	312
7	10–30	358.4	-5.0	11.0	-1.5	8.1	5.2	253
	90–120	358.0	-0.7	9.9	0.4	4.3	0.8	300
	185	100.8	-0.2	6.0	-1.9	2.3	1.9	186
8	302	109.8	-0.6	4.7	-0.4	4.4	0.7	236
9	22	120.5	-8.0	10.0	-9.4	11.8	12.3	220
	129–130	179.0	-6.9	8.0	-5.4	9.1	8.8	232

*Not included in Figure 6b.

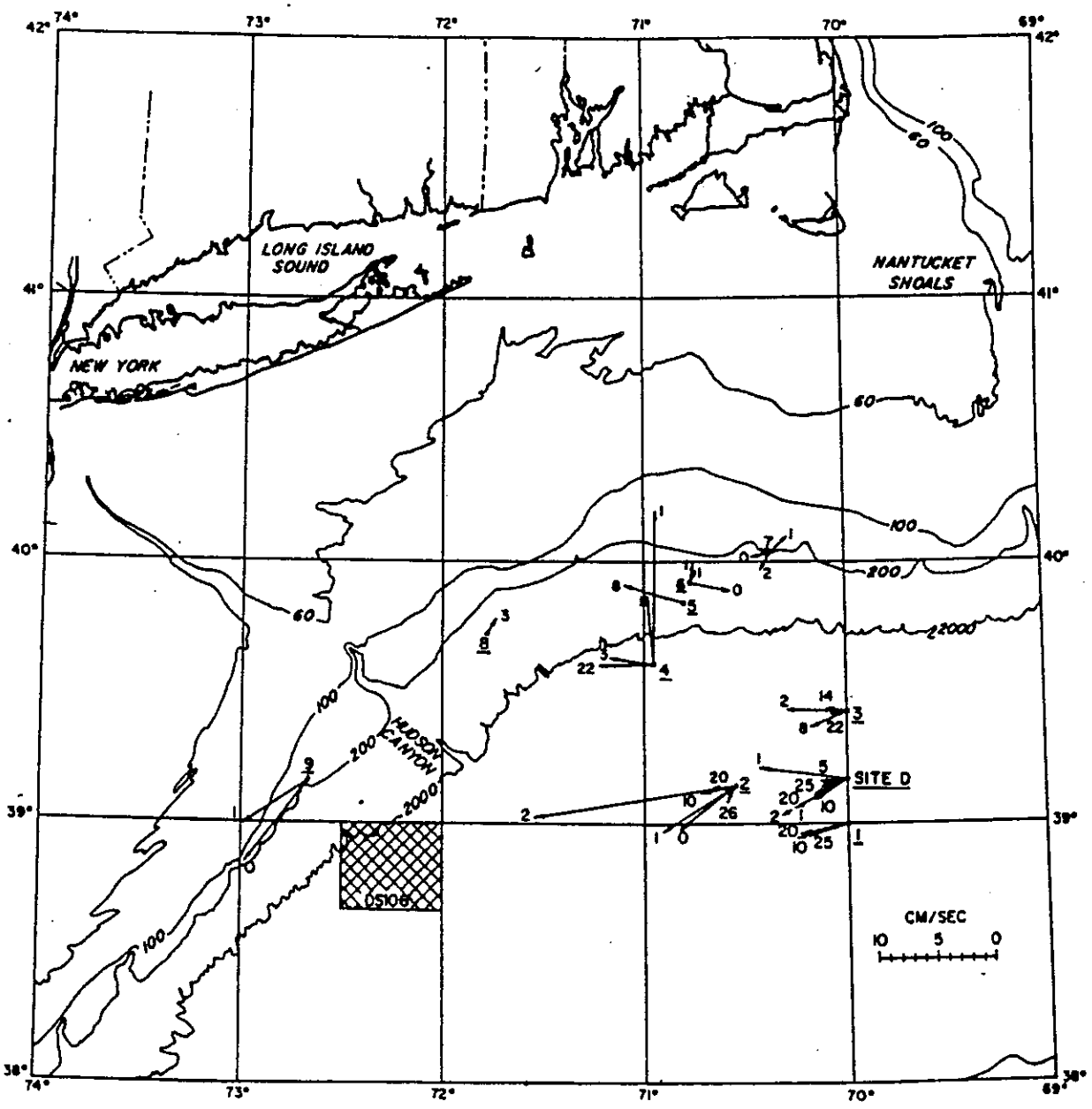

Figure 6a. Horizontally and vertically averaged current vectors within regions of similar water depth as given in Table 4a. The region number is underlined and the approximate depth (in hundreds of meters) is indicated for each vector.

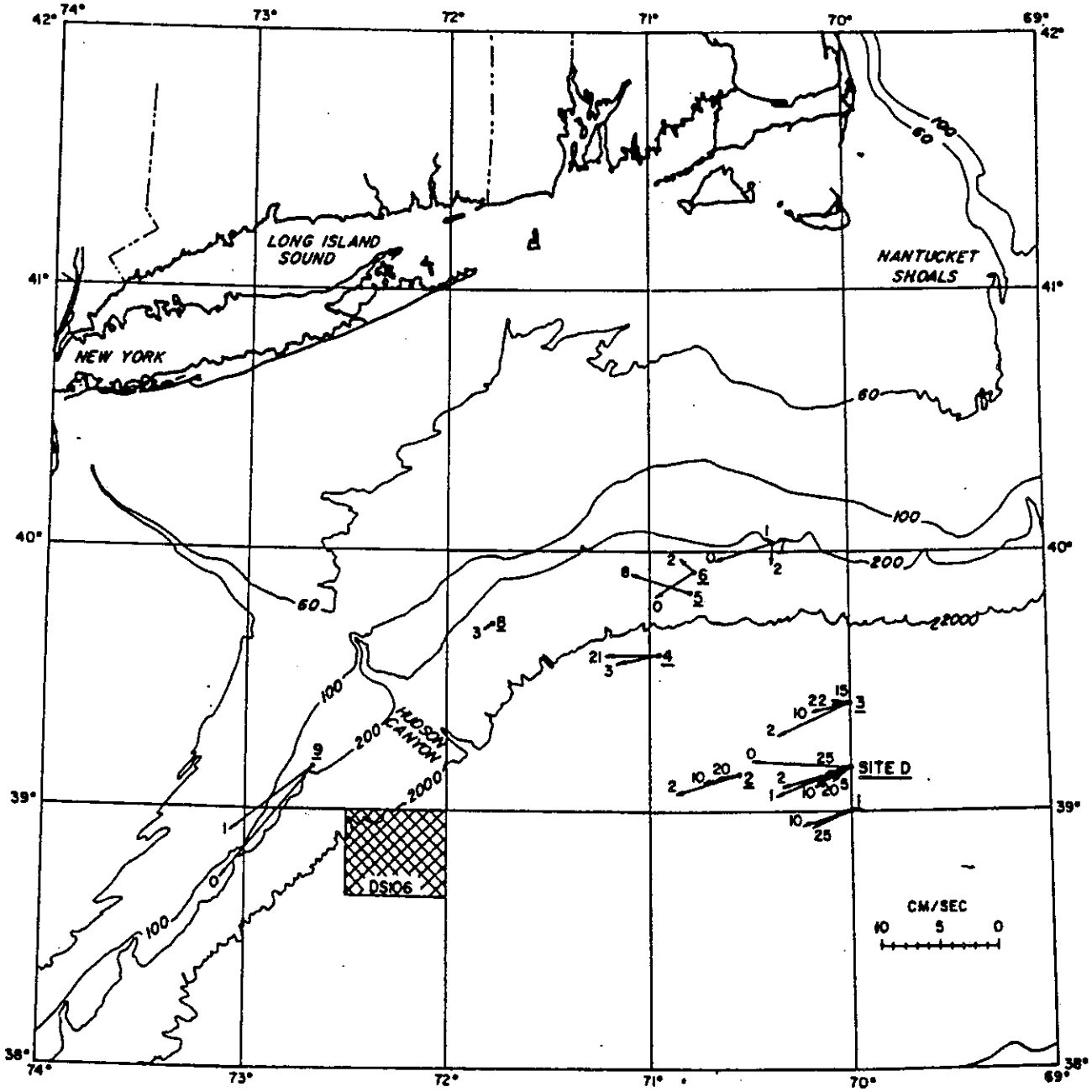

Figure 6b. Horizontally and vertically averaged current vectors within regions of similar water depth as given in Table 4b. The influence of warm rings has been removed. The region number is underlined and the approximate depth (in hundreds of meters) is indicated for each vector.

Figure 6a shows that, with some notable exceptions, the currents are generally westward and southwestward with speeds that decrease from the surface. The mean currents in Regions 2 and 4 are greater than 10 cm/sec but, in general, the mean currents in the various regions decrease from 6 or 7 cm/sec near the surface to 1 to 2 cm/sec below 1000 meters. The flow field with the influence of warm rings removed (depicted in Figure 6b) is more regular and does not have the large means associated with ring motion. In all cases, the velocities have a predominantly westward, along-isobath component. The mean, ring-free current at Site D at depths shallower than 1000 meters was 1 to 2 cm/sec lower. A comparison of the ring-free data with the averages from Webster (1969), which were based upon earlier data, shows that above 1000 meters Webster had higher means by 1 to 2 cm/sec while at 2000 meters the present results are higher by ~1.5 cm/sec.

The results from within 10 km of Site D, where about 40% of the data were collected, indicate that there is a counterclockwise veering of the current down to about 500 meters, below which there is a clockwise veering. This pattern is not consistently followed at nearby locations. The currents in Regions 6 and 7 remain somewhat anomalous even after the exclusion of the ring periods. A partial explanation for this behavior is that the measurements were made in the vicinity of the shelf/slope front, a region of strong shear and one which can be strongly influenced by atmospheric forcing. Thus, the available measurements may not give a complete representation of the currents. Lastly, the means from Region 9 at the head of Toms Canyon are notable for their relatively large magnitudes. Almost one-half year of data are included in each of the averages from Toms Canyon which should effectively average out fluctuations other than annual or interannual. The fact that the measurements were made over the winter months may be responsible for the high values, but sufficient data do not exist at the shelf edge to adequately describe the annual cycle.

In addition to the mean current field, a description of current fluctuations is required to understand the dispersion of material from DWD 106. The low-frequency fluctuations are characterized by the eddy kinetic energy (EKE), defined as the sum of the squares of the standard deviations ($\sigma_N^2 + \sigma_E^2$) of the north and east current components. The vertical distribution of the EKE, without regard to cross-slope location, is shown in Figure 7. As for the maximum observed currents, the largest values of the EKE are found above 200 meters. At this level, the background EKE (without rings) is typically between 100 and 300 cm^2/sec^2. This is about three times larger than the EKE at levels below 200 meters. Those records with warm ring contamination are distinguished in Figure 7; it is clear that the rings increase the EKE by a factor of 3 to 6, depending upon the percentage of the total record occupied by the high ring currents.

If the fluctuations in the slope region were isotropic, the distribution of the EKE would give all the information necessary about the oscillatory flow. In fact, however, the low-frequency motion of the slope is not isotropic and the along- and cross-isobath motions can differ significantly. Figure 8 shows the vertical distribution of the ratio of the eastward constituent of EKE (σ_E^2) to the northward constituent (σ_N^2), differentiating between those records with and without warm ring influence. For isotropic motion, the ratio would be one. In the upper 200 meters, there is a significant difference in the value of the ratio for periods with and without warm

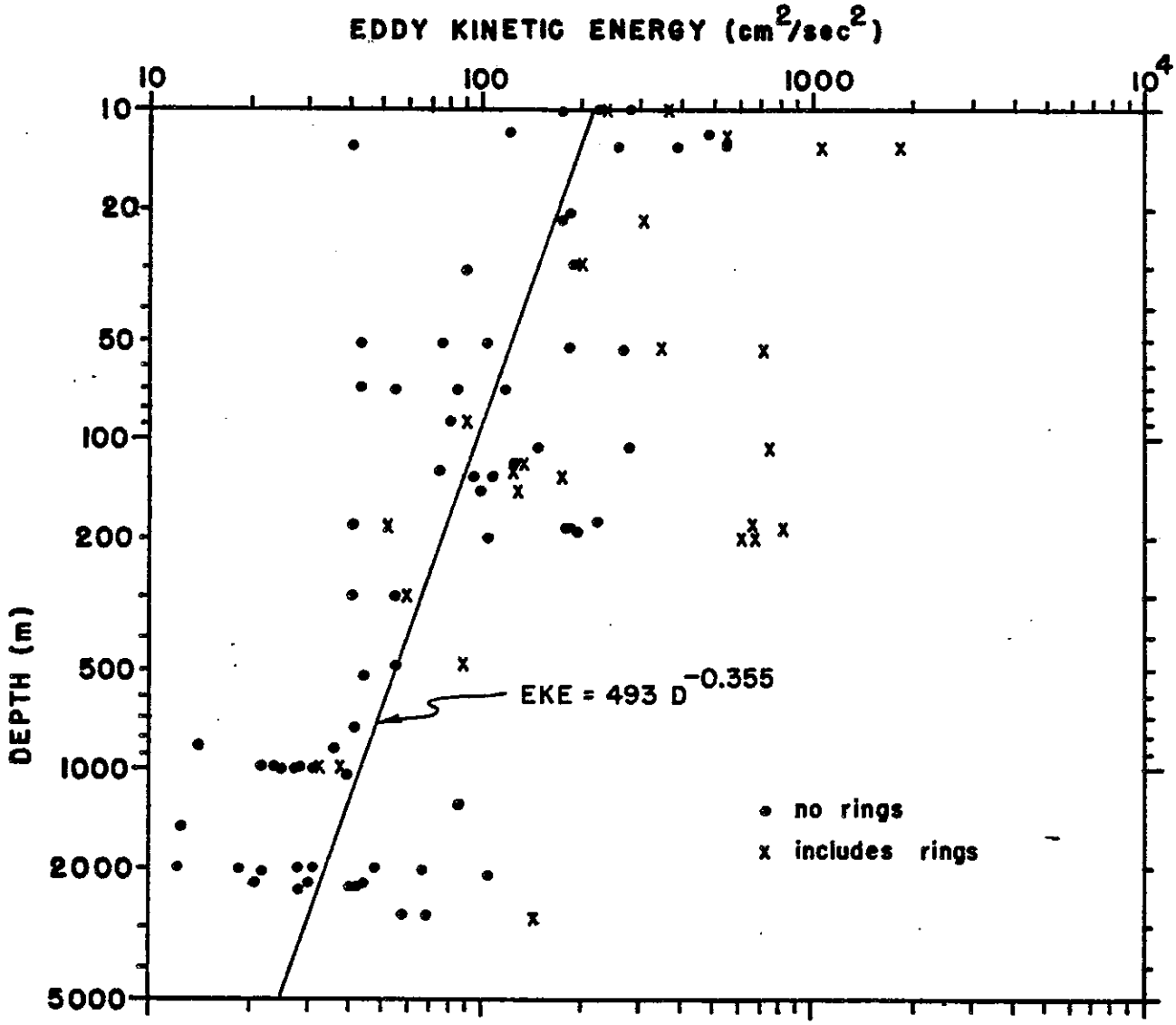

Figure 7. Vertical distribution of the low-frequency eddy kinetic energy (EKE) defined as $(\sigma_E^2+\sigma_N^2)$ without regard to the location of the data. Those records with warm ring influence are highlighted. Note the scale change in both axes.

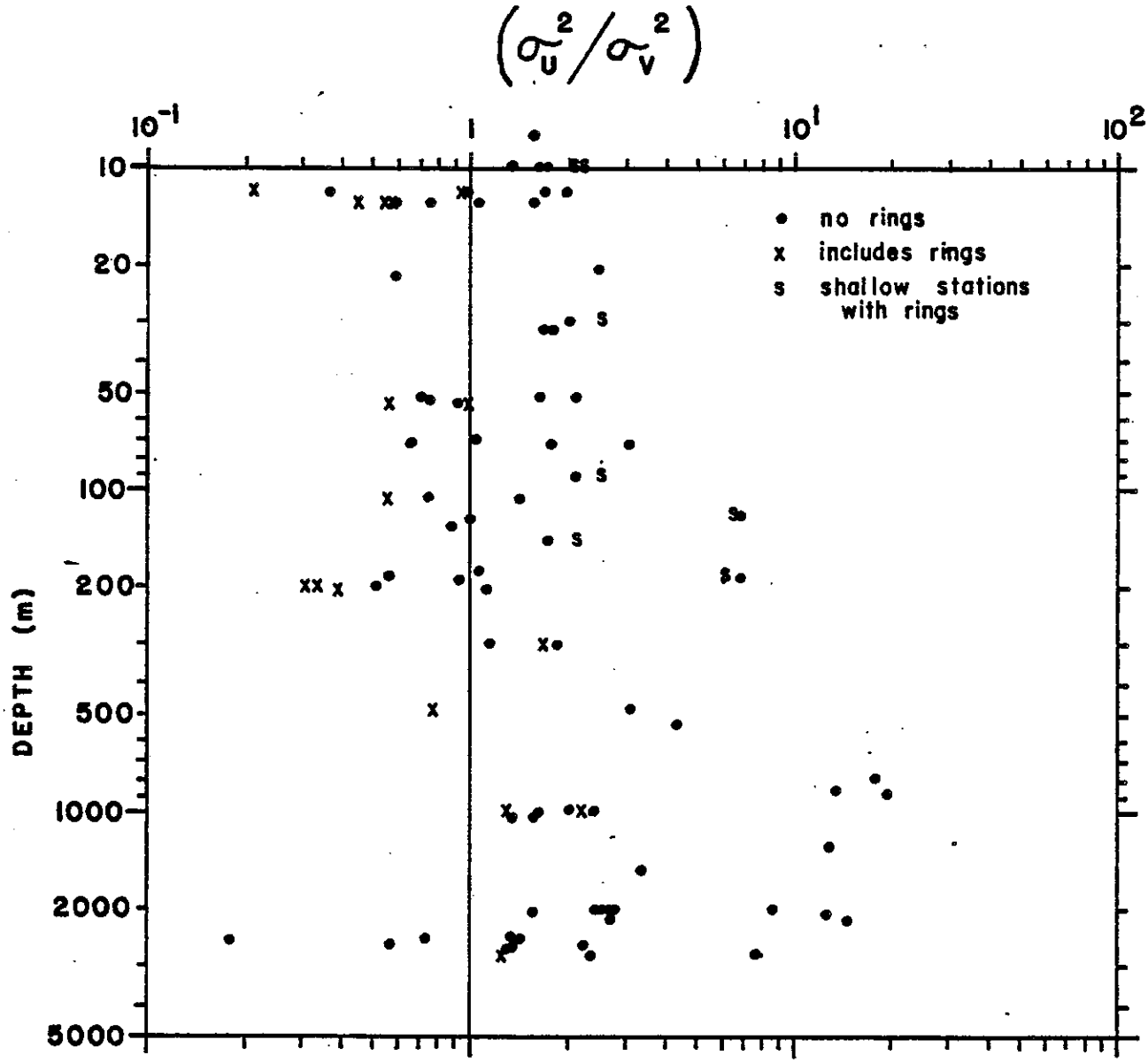

Figure 8. Vertical dependence of the polarization of the low-frequency eddy kinetic energy (EKE) defined as the ratio of the eastward constituent (σ_E^2) to the northward constituent (σ_N^2). Note the scale change in both axes.

rings. In the presence of warm rings, the ratio is more often less than one, while without the rings, the ratio tends to be greater than one. A ratio less than one at these station locations indicates cross-isobath polarization of the low-frequency currents during the passage of warm rings. This is due, at least in part, to the characteristic ring signature of north-south surges at Site D, which appears to dominate the statistics of ring passages in this data set. Stations closer inshore are characteristically polarized along-isobath during warm ring passages. A ratio greater than one during ring-free periods indicates along-isobath polarization of the background low-frequency currents above 200 meters. Below 200 meters there is less difference between the ring and nonring periods; in both cases, the oscillations tend to be strongly along-isobath polarized.

Since none of the current data come from the DWD 106 area and, in fact, as Table 2 shows, there is little data from the water depths characteristic of the dumpsite, the question naturally arises as to how to extend the available data to this region. For this purpose, the cross-isobath dependence of the mean onshore and isobath-parallel current components and the EKE are examined for six instrument depth ranges (0-50 m, 50-200 m, 200-500 m, 500-1000 m, 1000-2000 m, and >2000 m). Positive isobath-parallel currents are generally eastward or northeastward. The orientation of the coordinates for each station was determined by the shortest distance to the 200-meter isobath. For most of the records, this meant that the components remained east and north for the isobath-parallel and onshore directions, respectively.

Figures 9a through 9f present all three parameters as a function of distance from the 200-meter isobath. The considerable scatter seen in these plots is a reflection of some of the relatively short record lengths in the data set with lower statistical stability and also the effect of annual and longer term fluctuations which can bias the records. The scatter is greatest above 200 meters. Visual identification of a cross-isobath dependence from the plots is made difficult by the scatter, except in a few instances. To formalize the procedure, linear regressions were calculated for each variable, the results of which are presented in Table 5. There was a significantly nonzero linear offshore dependence in only one-third of the cases at the 90% confidence level. Thus, for most situations, a simple horizontal average is the best estimator for DWD 106. A notable exception is the isobath-parallel current component above 200 meters which shows a significant increase in westward and southwestward flow offshore on the order 5 cm/sec per 100 km. In only one instance did the onshore flow exhibit a significant cross-isobath dependence, and that indicated a decrease offshore. For the two cases where the EKE regression showed a significant offshore dependence, the EKE increased offshore. This dependence is not surprising since the Gulf Stream is a major source of low-frequency energy (Thompson, 1978; Hogg, 1981).

4.2 Annual Variability

The analysis presented in the previous section was conducted without regard for the time of the year when the data were obtained. For most of the locations, the data covered only a small portion of a year, which inevitably increased the error bounds on estimates of the mean currents in the presence of an annual fluctuation. At Site D, however, there is sufficient high-quality data in each month to attempt to determine the annual cycle, if one

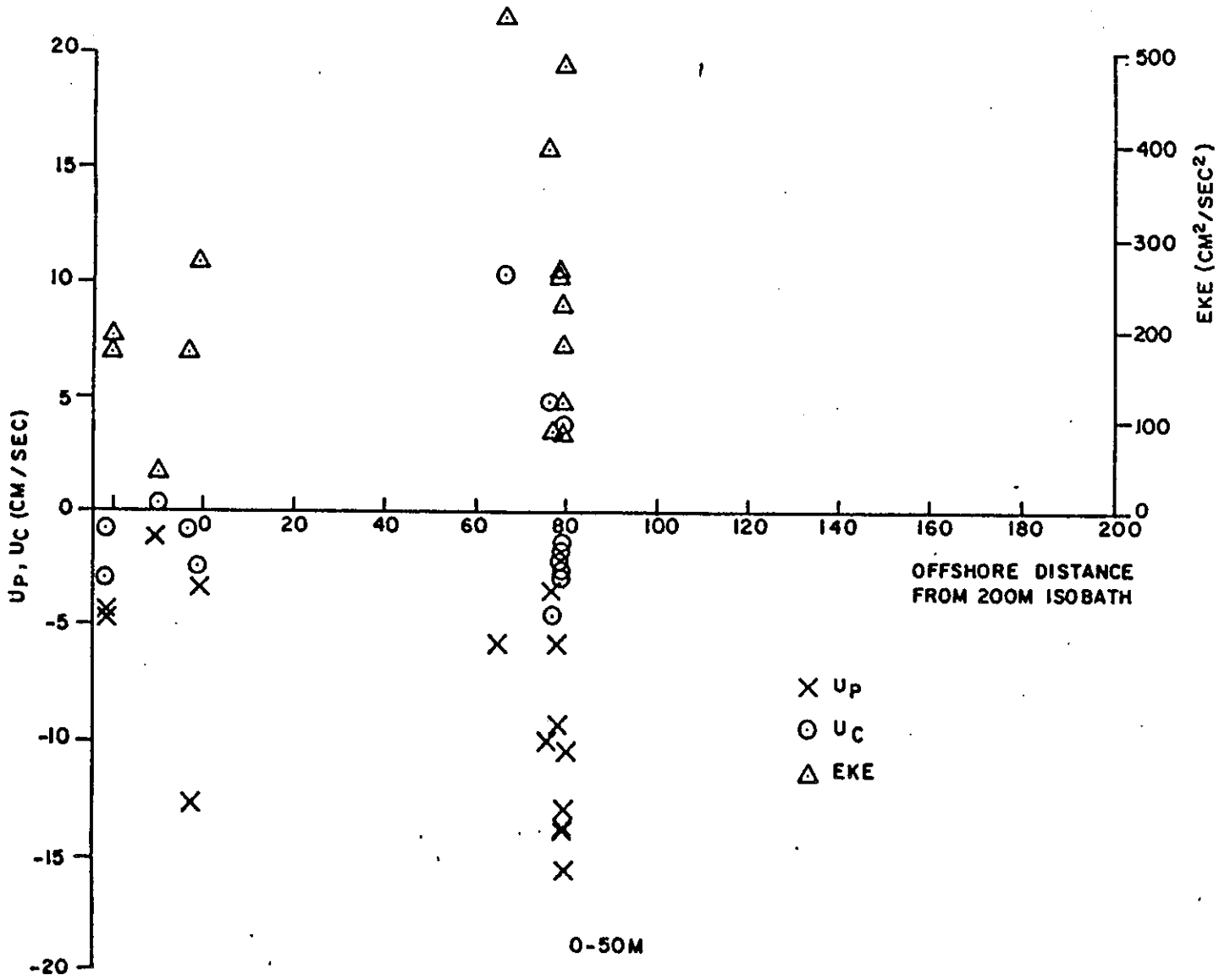

Figure 9a. Cross-isobath dependence of current components, U_P (isobath-parallel) and U_C (cross-isobath), and eddy kinetic energy (EKE) for the depth range 0 to 50 meters.

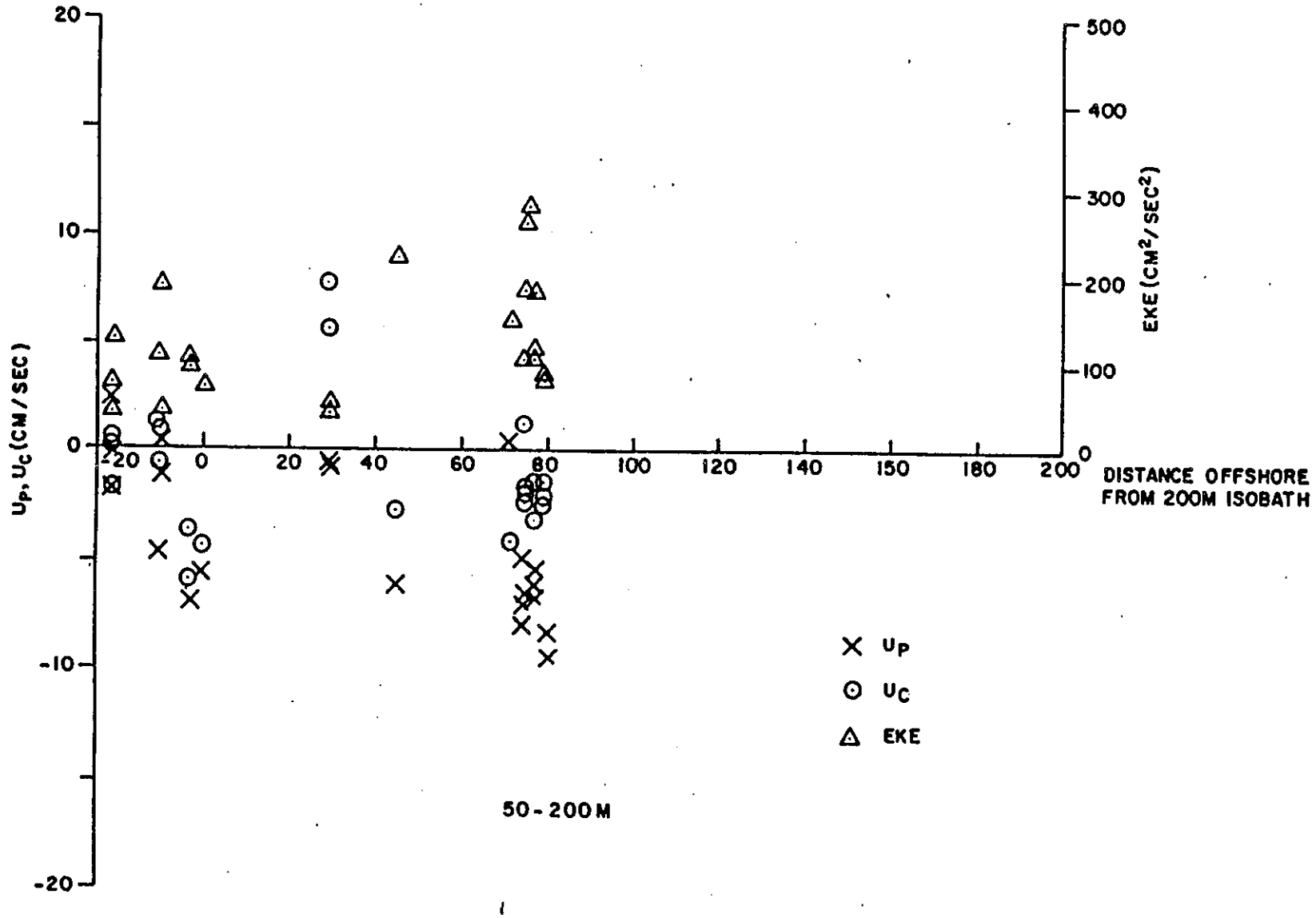

Figure 9b. Cross-isobath dependence of current components, U_P (isobath-parallel) and U_C (cross-isobath), and eddy kinetic energy (EKE) for the depth range 50 to 200 meters.

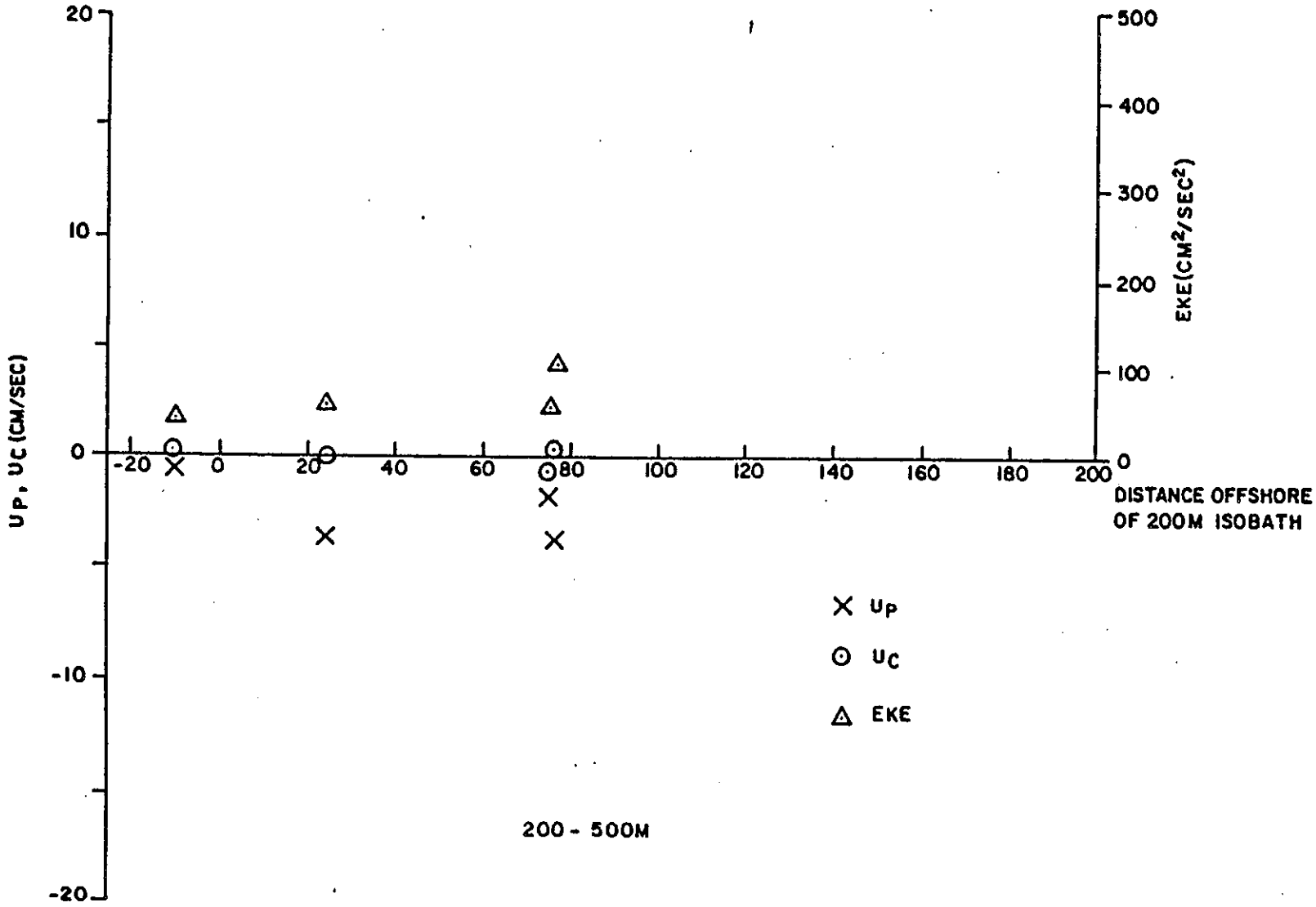

Figure 9c. Cross-isobath dependence of current components, U_P (isobath-parallel) and U_C (cross-isobath), and eddy kinetic energy (EKE) for the depth range 200 to 500 meters.

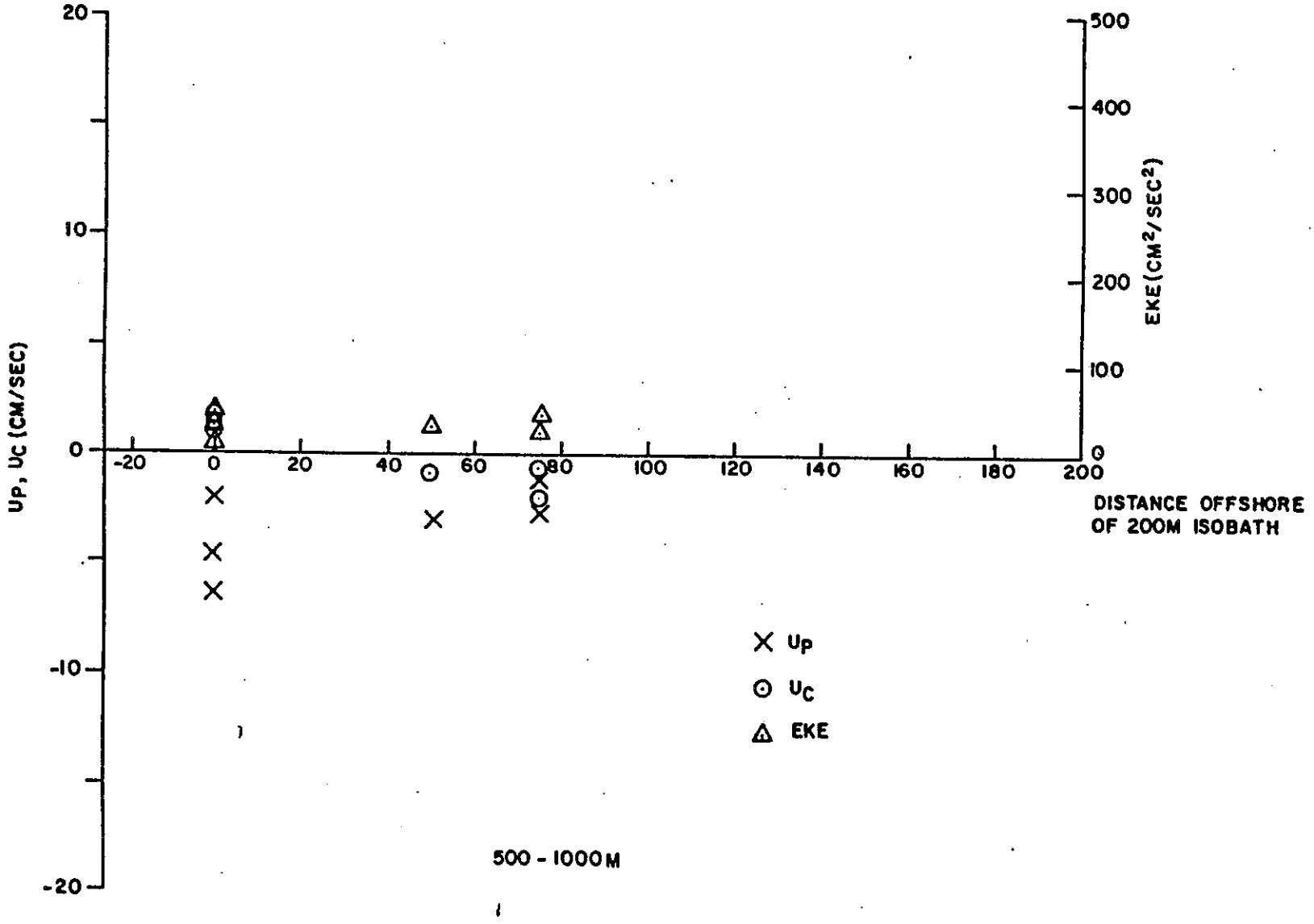

Figure 9d. Cross-isobath dependence of current components, U_P (isobath-parallel) and U_C (cross-isobath), and eddy kinetic energy (EKE) for the depth range 500 to 1000 meters.

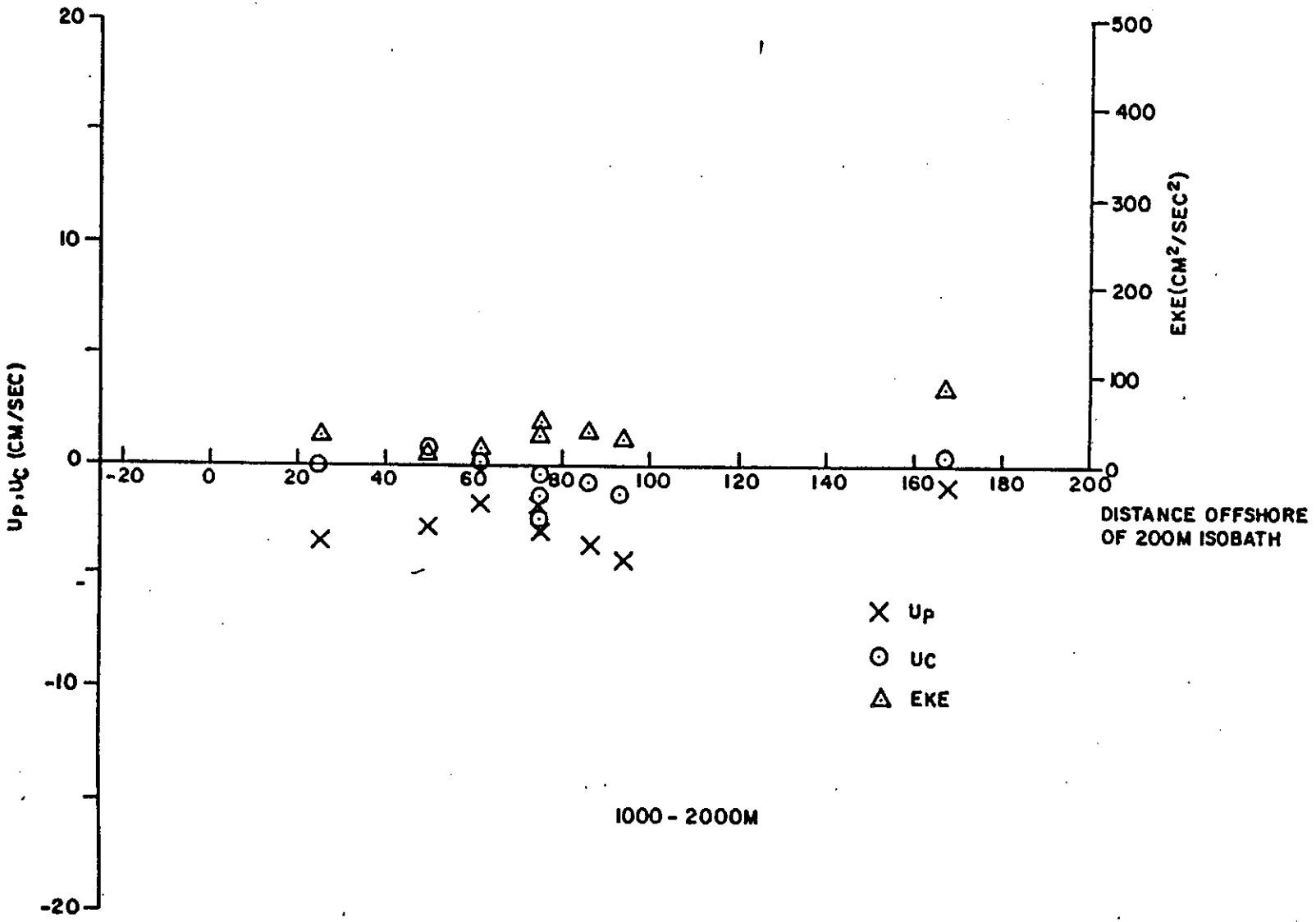

Figure 9e. Cross-isobath dependence of current components, U_P (isobath-parallel) and U_C (cross-isobath), and eddy kinetic energy (EKE) for the depth range 1000 to 2000 meters.

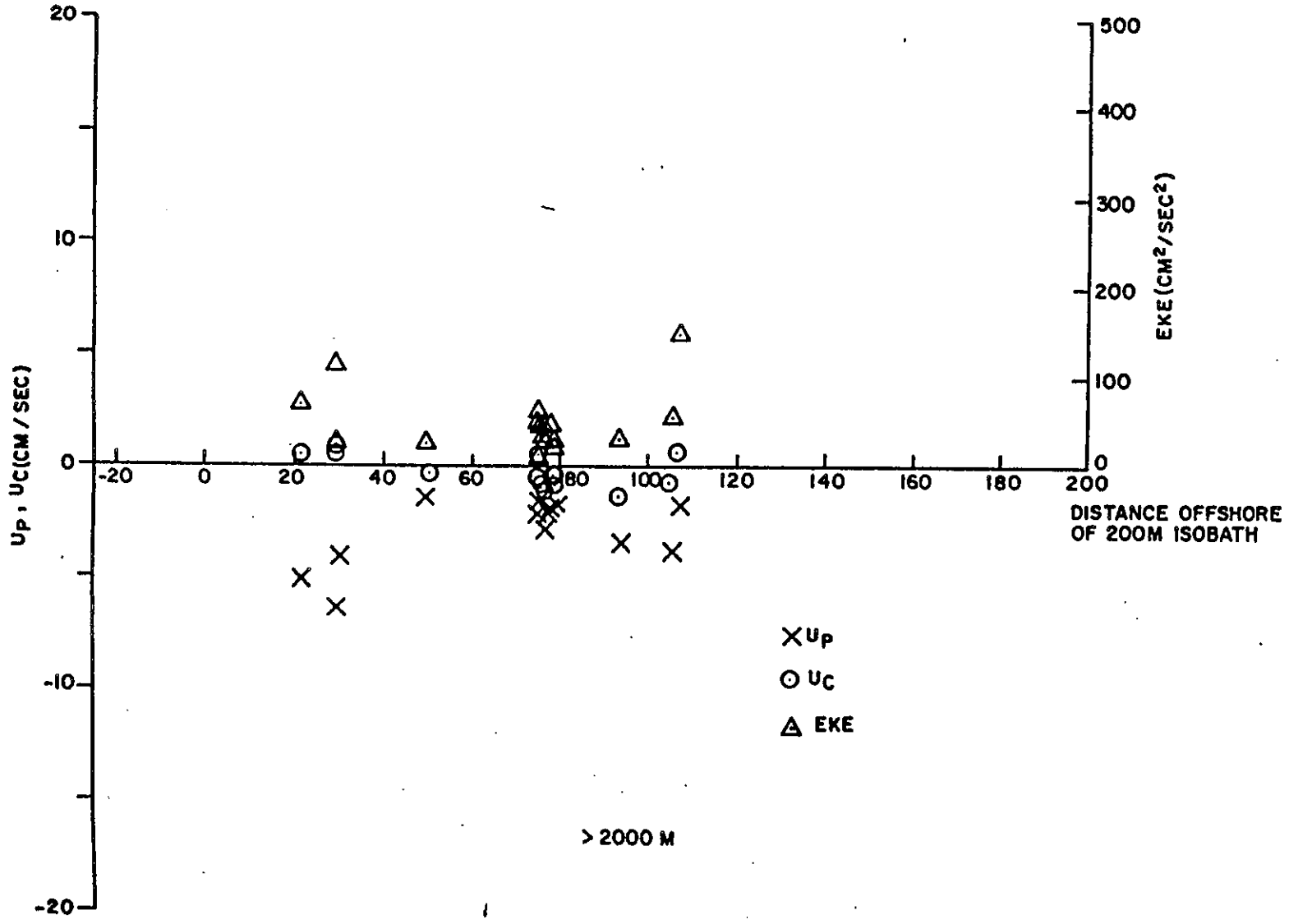

Figure 9f. Cross-isobath dependence of current components, U_P (isobath-parallel) and U_C (cross-isobath), and eddy kinetic energy (EKE) for depths greater than 2000 meters.

Table 5. Linear dependence of current components, U_P (isobath-parallel) and U_C (cross-isobath), and eddy kinetic energy (EKE) on cross-isobath distance, D, in kilometers. $[U_P, U_C, EKE] = a + b \cdot D$. Data from 200 to 500 meters have not been included because of insufficient data and the permanent thermocline in this depth range.

Depth (m)		a	b
0–50	U_P	-5.737	-0.058[1]
	U_C	-0.905	0.015
	EKE	189.299	0.939
50–200	U_P	-2.647	-0.047[1]
	U_C	-0.643	-0.011
	EKE	101.223	0.686[2]
500–1000	U_P	-4.357	0.030
	U_C	1.424	-0.038[2]
	EKE	30.497	0.040
1000–2000	U_P	-3.102	0.006
	U_C	-0.454	-0.001
	EKE	-5.578	0.484[1]
>2000	U_P	-4.914	0.035[2]
	U_C	0.307	-0.010
	EKE	52.652	-0.042

[1]Significant at 95%

[2]Significant at 90%

exists. For this purpose, monthly averages of all the records free of warm rings were calculated for the east and north velocity components and the eddy kinetic energy. Above 1000 meters the temporal coverage of the data was discontinuous, even at Site D, so that there were a few months with little or no data. The analysis included only those months having at least a month of data in the average, with the exception of December for the depth range 0 to 50 meters which had 28.5 days of data. All the monthly averages were given equal weight, even though there was a variable amount of data in each.

Plots of the monthly mean east (U) and north (V) currents and the EKE at five depth levels from Site D (0-50 m, 200 m, 1000 m, 2000 m, and 2500 m) are shown in Figures 10a through 10e. In addition, the monthly averages were fitted, in a least-squares sense, to a mean plus an annual sinusoid using the method of Fofonoff and Bryden (1975). The results of the calculation are shown in Table 6.

In the upper 50 meters, Figure 10a illustrates that there is a strong annual signal for the east current component, U, a weaker signal for the northward component, V, and a great deal of variability in the EKE. The east component, which is basically along-isobath, has a minimum westward velocity of between 2 and 3 cm/sec in spring and a maximum of between 12 and 14 cm/sec in fall. Table 6 indicates that the east component has a mean of -8.5 cm/sec ($\pm$6 cm/sec), with the minimum in April and the maximum in October. The north component in the upper 50 meters is generally southward and offshore during the winter and spring, and northward and onshore in the late summer and fall. The least-squares analysis indicates that the annual change in the north component is about the same as for the east component, $\pm$5.6 cm/sec, but that the mean is much smaller and not significantly different from zero. Figure 10a shows that the large calculated annual signal in the north component may be the result of October's high current. Without that data point the north-south oscillation would be reduced to 2 to 3 cm/sec, but the phase would be about the same, i.e., offshore in winter/spring and onshore in summer/fall. The EKE in the upper layer has a mean of about 200 cm^2/sec^2 and is quite variable from month to month with the result that there is no statistically significant annual EKE signal.

Monthly current components at 200, 1000, 2000, and 2500 meters do not show the consistent annual variability that is seen at the surface. Figure 10b and Table 6 show a significant annual variation only in the V-component of velocity at 200 meters; Figures 10c and 10d and Table 6 show a significant annual variation only in the EKE at 1000 and 2000 meters; Figure 10e and Table 6 show no significant annual variation in any of the parameters at 2500 meters.

The strong annual signal for both current components between 0 and 50 m makes it tempting to look for a cause. Figure 11 shows a least-squares prediction of the annual wind stress cycle adapted from the analysis of Butman and Beardsley (1984). Their calculations indicate that the eastward stress, τ_E, has annual and semiannual components of about the same magnitude, while the north component, τ_N, is dominated by the annual signal. The eastward wind stress, on a monthly basis, is fairly small but is positive for the first two-thirds of the year, decreasing to just less than zero in October. If the coastal constraint of zero normal flow applies to the slope waters, then it is reasonable to expect the east current component of the slope waters above the

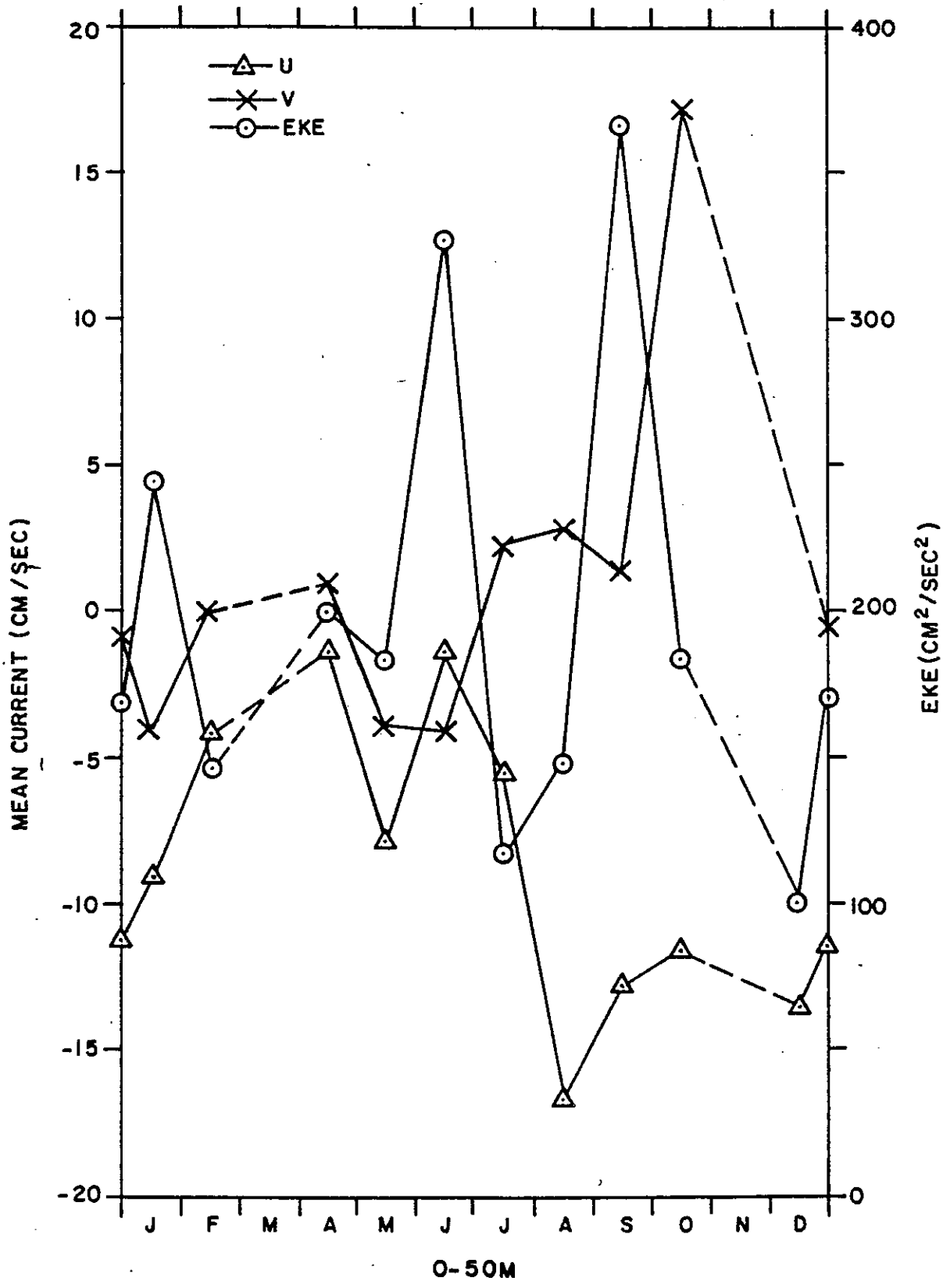

Figure 10a. Monthly mean east (U) and north (V) components of current and eddy kinetic energy (EKE) for the depth range 0 to 50 meters.

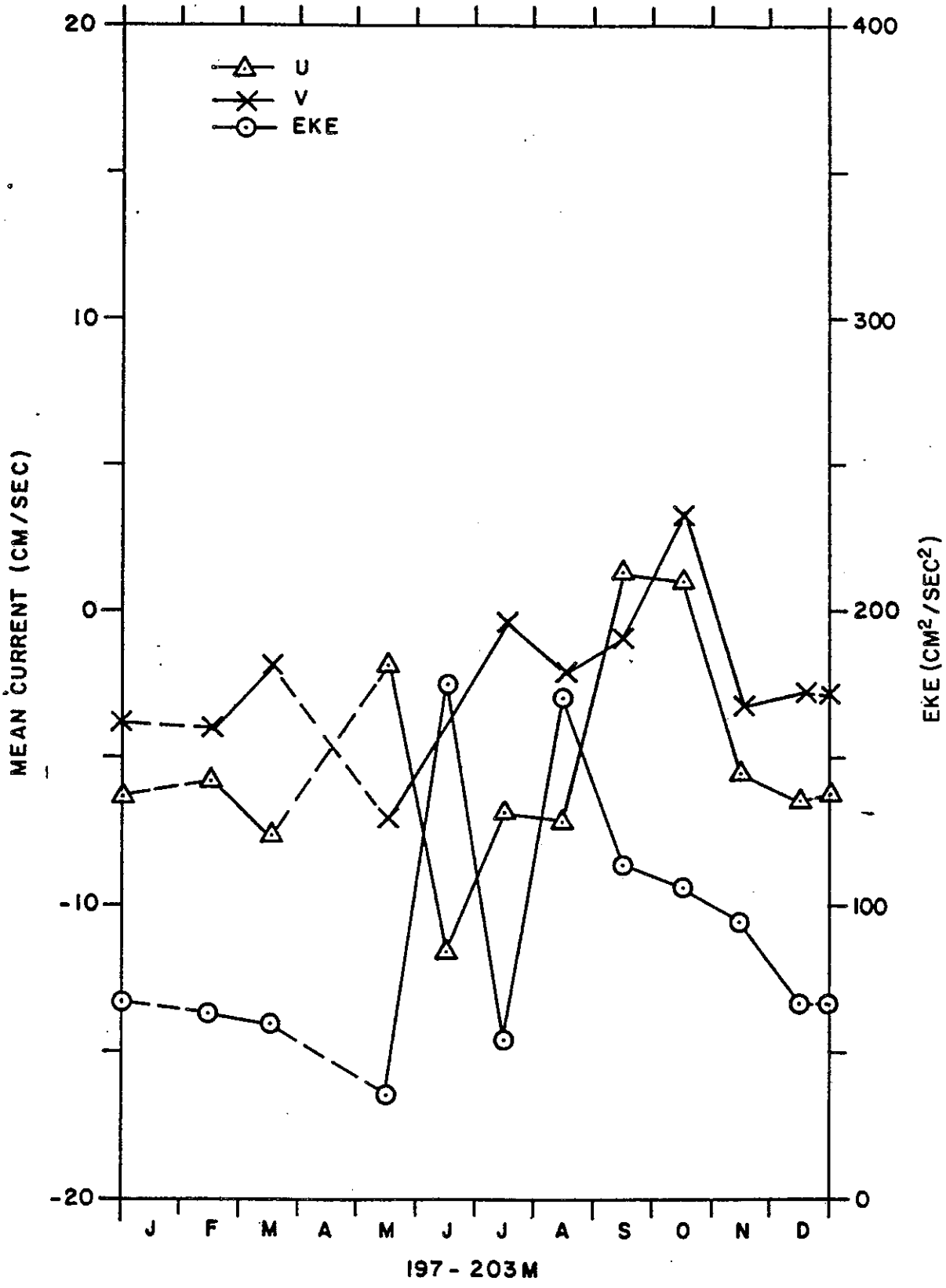

Figure 10b. Monthly mean east (U) and north (V) components of current and eddy kinetic energy (EKE) at 200 meters.

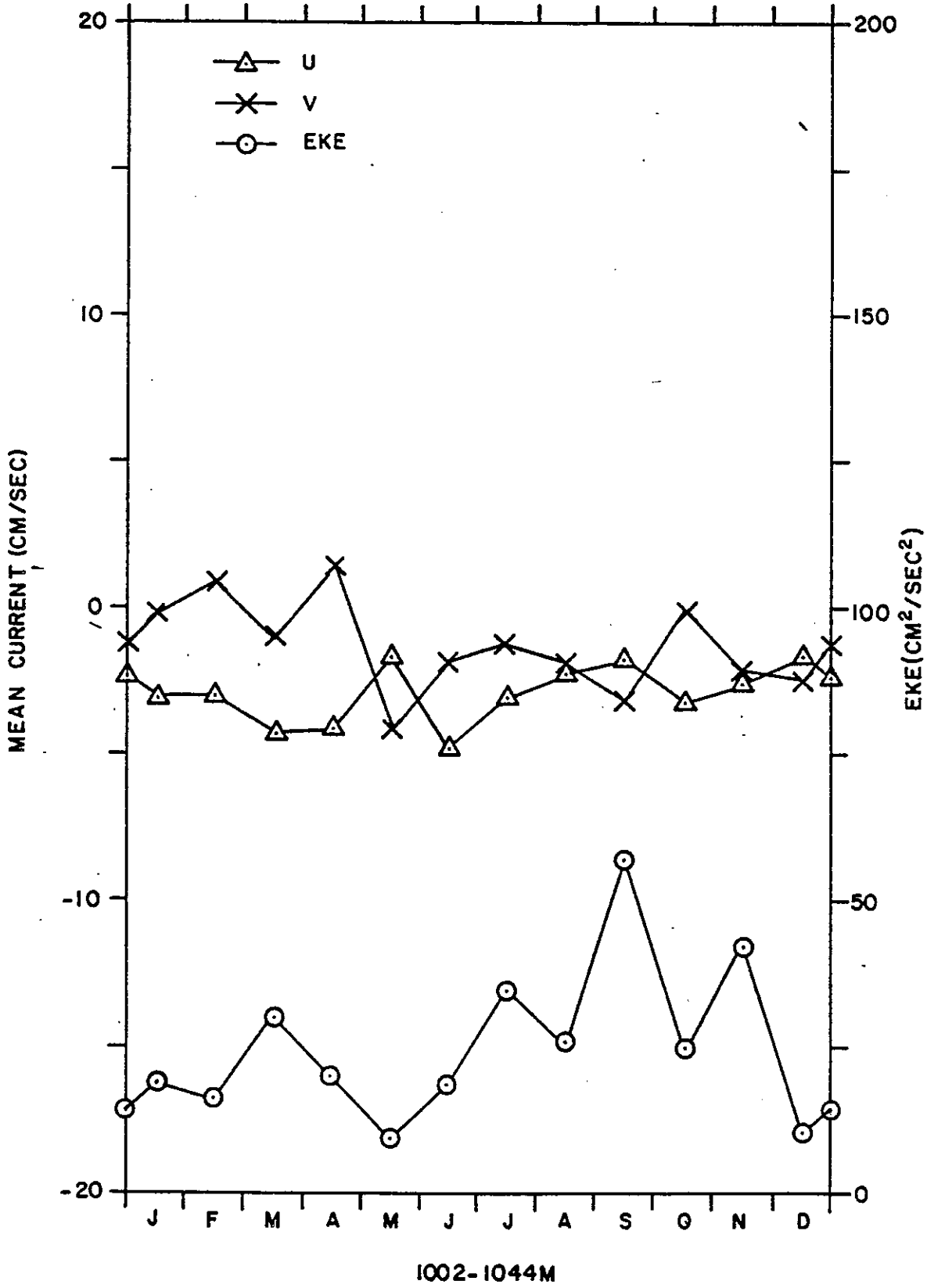

Figure 10c. Monthly mean east (U) and north (V) components of current and eddy kinetic energy (EKE) at 1000 meters.

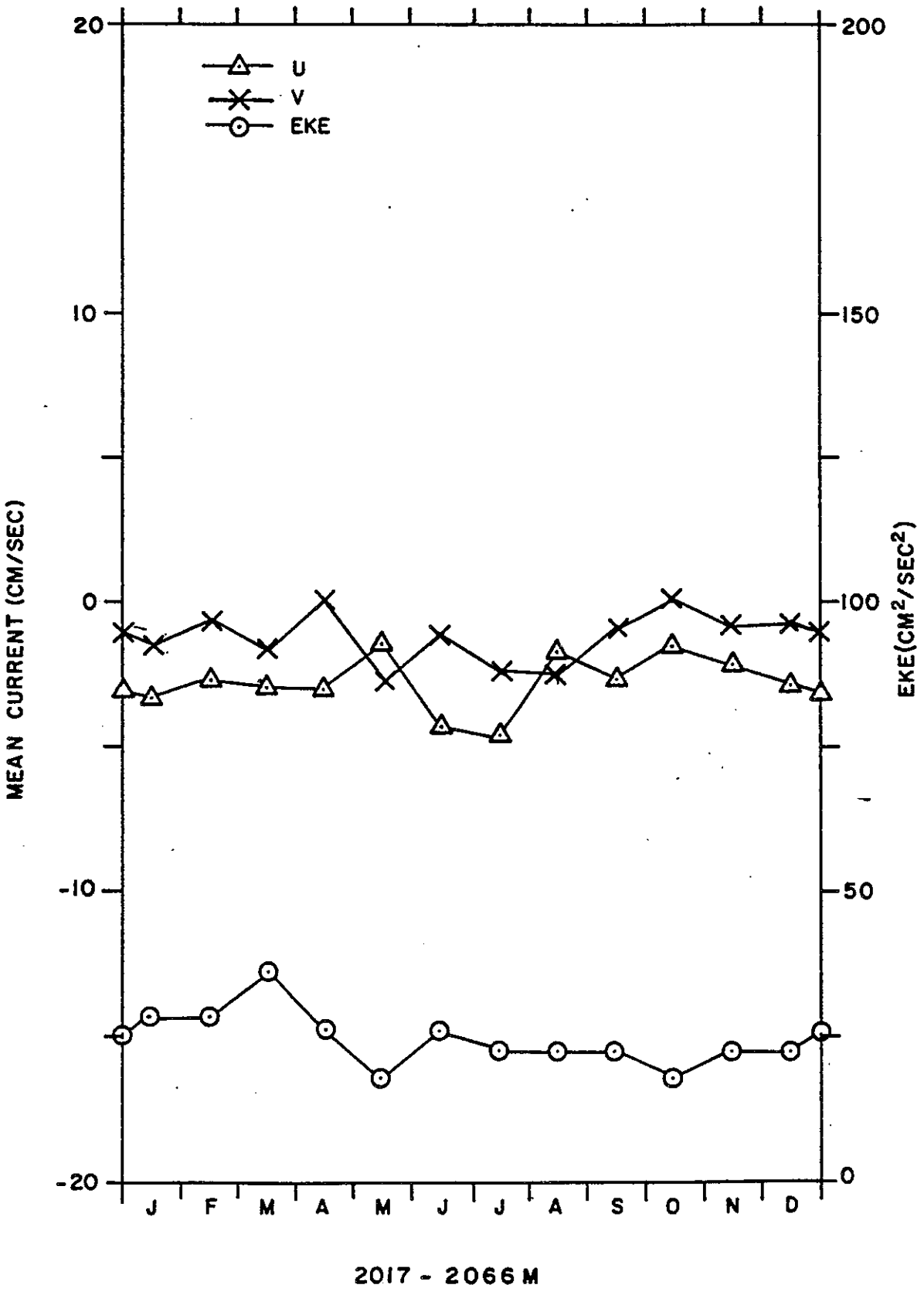

Figure 10d. Monthly mean east (U) and north (V) components of current and eddy kinetic energy (EKE) at 2000 meters.

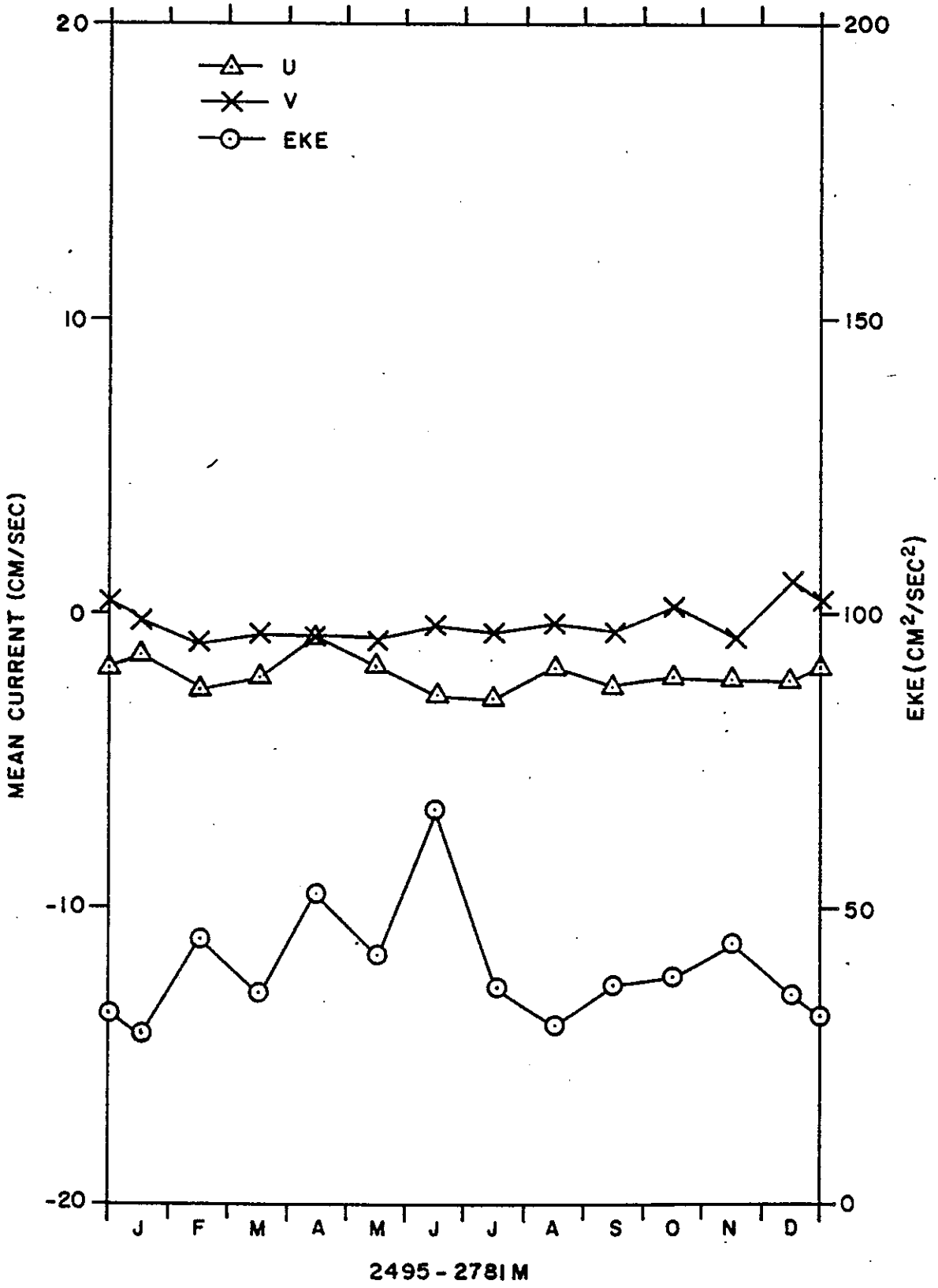

Figure 10e. Monthly mean east (U) and north (V) components of current and eddy kinetic energy (EKE) at 2500 meters.

Table 6. Least squares fit of monthly current components to an annual mean and annual sinusoid using the method of Fofonoff and Bryden (1975).

$$[U, V, EKE] = b_1 + b_2 \sin(2\_t/12) + b_3 \cos(2\_t/12)$$
$$= b_1 + A \cos(2\_t/12 - \emptyset)$$

Depth (m)	Variable	b_1	b_2	b_3	A	$\emptyset$ (deg)
0-50	U	-8.47 ± 2.18^1	5.07 ± 3.15^1	-3.18 ± 3.00^1	$5.98^{+4.30}_{-4.06}$	$122.1^{+40.6}_{-30.8}$
	V	1.46 ± 3.22	-4.91 ± 4.65^1	2.80 ± 4.42	$5.65^{+6.33}_{-4.01}$	$-60.3^{+58.2}_{-110.6}$
	EKE	198.47 ± 58.33^1	-19.22 ± 84.35	-20.20 ± 80.60	n.s.	n.s.
200	U	-5.28 ± 2.49^1	-2.13 ± 3.51	1.46 ± 3.46	n.s.	n.s.
	V	-2.58 ± 1.47^1	-2.15 ± 2.08^1	0.92 ± 2.03	$2.34^{+2.82}_{-1.42}$	$-66.8^{+65.5}_{-109.6}$
	EKE	88.67 ± 27.54^1	-34.70 ± 38.89	-14.26 ± 38.21	n.s.	n.s.
1000	U	-2.99 ± 0.51^1	-0.60 ± 0.72	0.42 ± 0.71	n.s.	n.s.
	V	-1.40 ± 0.84^1	0.88 ± 1.20	0.48 ± 1.20	n.s.	n.s.
	EKE	25.58 ± 6.66^1	-10.68 ± 9.42^1	0.77 ± 9.42	$10.71^{+11.83}_{-9.23}$	$274.1^{+78.8}_{-85.8}$
2000	U	-2.77 ± 0.49^1	-0.25 ± 0.71	0.37 ± 0.70	n.s.	n.s.
	V	-1.23 ± 0.45^1	0.03 ± 0.67	0.58 ± 0.63	n.s.	n.s.
	EKE	24.42 ± 2.19^1	4.38 ± 3.10^1	0.83 ± 3.10	$4.46^{+3.99}_{-2.93}$	$79.3^{71.3}_{-61.2}$
2500	U	-2.16 ± 0.30^1	0.30 ± 0.42	0.14 ± 0.44	n.s.	n.s.
	V	-0.51 ± 0.29^1	-0.16 ± 0.41	0.36 ± 0.41	n.s.	n.s.
	EKE	41.13 ± 5.37^1	2.86 ± 7.60	-6.09 ± 7.60	n.s.	n.s.

[1]Significant at 90%
n.s. - not significant

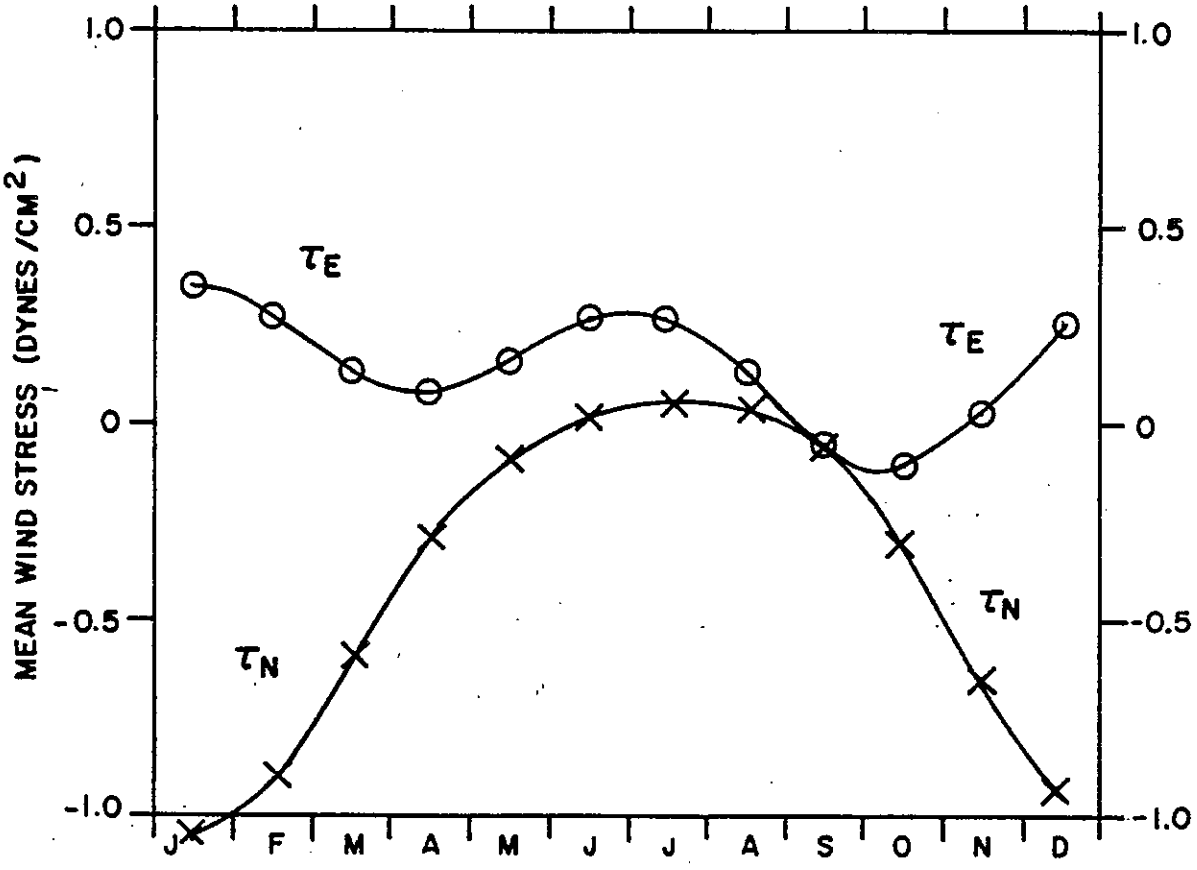

Figure 11. East (τ_E) and north (τ_N) components of wind stress calculated by a least-squares fit of data from Nantucket Lightship according to the analysis of Butman and Beardsley (1984).

thermocline to be in phase with the wind stress. Roughly, this is true with a minimum westward flow in the winter and spring corresponding to the period of larger eastward wind stress and a maximum westward current in the later summer and fall when the eastward stress is at a minimum. However, the magnitude of the monthly mean eastward wind stresses is small (roughly 0.2 dynes/cm^2) and cannot account for the large eastward current fluctuations on the order of 11 cm/sec.

5. ANALYSIS OF ADVECTION CHARACTERISTICS

5.1 Eulerian Data

Additional circulation characteristics within the slope region have been examined using selected near-surface Eulerian data sets in an attempt to provide a further description of the current field in terms directly related to the advection of pollutants. The data sets of interest were collected in the general vicinity of Site D at depths of 50 meters or less and cover the period from August 1968 to July 1972. The analysis is limited to the portions of each record found to be free of the effects of warm core rings, as described in the previous section. The current characteristics addressed in this analysis include the following:

1) low current speed incidence and persistence,
2) residence time,
3) stagnation periods,
4) on-shelf motion, and
5) recirculation.

The occurrence of low current speeds is of obvious relevance, especially in cases where the currents remained low for extended periods of time. Consequently, each of the selected data sets was analyzed to estimate the incidence of current speeds below 5 and 10 cm/sec. The mean persistence associated with each current speed was also estimated by determining the total duration of the record where the speed fell below the specified level and dividing by the number of discrete excursions below this level. The results of this analysis are shown in Table 7. At depths above the seasonal thermocline (0 to 30 meters), low current speeds are relatively infrequent. The results from the shorter records taken during the late spring and summer indicate higher incidence and persistence levels, consistent with the annual minimum current period determined from the analysis in Section 6. The results from the deeper instruments (30 to 50 meters) also reflect this tendency. Although the overall persistence estimates for the two categories follow a reasonable trend, it should be emphasized that the persistence of individual low current speed events was found to be highly variable. This is particularly evident from the results obtained for Station 15. The averages should be interpreted with this variability in mind.

Residence time was estimated by examining progressive vector plots of low-pass-filtered data (with eddy periods deleted) on a weekly basis and recording the time required for a water parcel originally at the center of an area the size of DWD 106 to move outside of its boundaries. Table 8 lists

Table 7. Persistence of near-surface currents in the slope region. The positions of the individual current meter stations are given in Figure 2..

Station	Inst. Depth (m)	Time Interval	Current Speed Incidence (%) <5 cm/s	Current Speed Incidence (%) <10 cm/s	Current Speed Persistence (hrs) <5 cm/s	Current Speed Persistence (hrs) <10 cm/s
Category 1: 0-30 M						
13	12	6/29-8/17/70	17.6	48.2	29	51
26	12	4/29-5/23/71	8.5	28.7	12	40
29	12	4/29-5/23/71 7/29-8/5/71	22.0	51.3	23	76
1	13	8/24-11/27/68 12/21-12/30/68 6/9-8/10/69 10/8-10/18/69	2.4	11.2	15	32
2	13	6/15-8/10/69 10/8-10/16/69	1.1	7.6	18	30
			4.8	15.3	21	44
Category 2: 30-54 M						
14	32	6/29-8/17/70	14.5	50.3	42	83
15	32	6/30-8/18/70	31.1	60.6	60	232
41	53	12/14-1/2/72 1/24-3/3/72 4/3-7/14/72	12.0	36.3	26	53
3	54	8/24-10/1/68 12/21-3/5/69 6/15-8/10/69 10/8-10/17/69	4.7	22.8	34	58
			11.3	34.9	35	68

Table 8. Residence time estimates and incidence of stagnant currents in the near-surface slope waters. The positions of the individual current meter stations are given in Figure 2.

Station	Inst. Depth (m)	Time Interval	Mean Residence Time (days)	Incidence of Stagnant Conditions (%)
Site D				
13	12	6/70-8/70	3.7 ± 3.4	57
1	13	8/68-11/68 6/69-8/69	1.7 ± 1.0	18
2	13	6/69-8/69	1.6 ± 0.8	23
14	32	6/70-8/70	3.9 ± 2.2	41
15	32	6/70-8/70	5.1 ± 5.7	59
3	54	8/68-10/68 12/68-3/69	2.2 ± 1.7	31

the residence time estimates determined in this manner from the selected near-surface records. The results are seen to be highly variable, as might be expected, with the mean residence time falling within the range from roughly one to five days.

Stagnant conditions are defined as those periods during which a progressive vector track remained within an area the size of DWD 106 for five days or more. Note that residence time was based on virtual displacement starting from the center of the dumpsite area, while stagnation periods correspond to displacements from boundary to boundary. Typically, stagnant conditions occurred between 17% and 31% of the time, based on the longer data records available from Site D.

Another question pertaining to waste accumulation is the recirculation of waters back through the dumpsite. This question was addressed by examining the progressive vector plots for periods when tracks left an imaginary area the size of DWD 106 and then returned to the area. Table 9 presents the results of this analysis. It is apparent that short-term recirculation of waters away from DWD 106 and back to the site is a rare occurrence, being observed on only two occasions within a period of roughly two years.

Periods of on-shelf motion were identified based on the progressive vector plots and are presented in Table 9 in terms of the percent time during which this condition existed at each station. The on-shelf (virtual) displacement was also determined for each period and the arithmetic average is included in the table. On-shelf motion was defined to include current directions between 315^{o} and 045^{o} true, as appropriate for the vicinity of Site D. An appropriate range for DWD 106 would lie roughly between 270^{o} and 360^{o}. The transferrence of results to the dumpsite is considered rather tenuous in the case of this particular statistic, and any quantitative application of the results should be made with caution. It is emphasized that this analysis applies to the current field in the absence of warm core rings.

In general, it is apparent that periods of on-shelf motion are not rare. Also, they are sufficiently persistent to produce substantial on-shelf displacements.

5.2 Lagrangian Data

It was originally intended to augment the Eulerian results by applying the same analysis procedures to Lagrangian data sets, specifically those drifter tracks identified in Section 3.3. However, a detailed assessment of the data revealed that this was not generally feasible. As previously noted, the number of drifter tracks available to describe the slope water region is quite limited. Also, each set of drifter tracks was found to have specific limitations which precluded a valid application of the analysis procedures used in the foregoing examination of the Eulerian data.

In reviewing the available Lagrangian data, it is apparent that the two drifters released by NOAA directly at DWD 106 are the most relevant to the present study. These were tracked daily by satellite over the period from 4 September to 31 December 1980. The drifters remained within the slope water over an initial 33-day period and then became entrained within the Gulf

Table 9. Recirculation and on-shelf motions in near-surface slope waters. The positions of the individual current meter stations are given in Figure 2.

Station	Inst. Depth (m)	Time Interval	Incidence of Recircula-tion (%)	Incidence of On-Shelf Currents (%)	Mean On-Shelf Displacement (km/day)
Site D					
13	12	6/70–8/70	4	15	6
1	13	8/68–11/68 6/69–8/69	0	14	21
2	13	6/69–8/69	0	45	17
14	32	6/70–8/70	0	14	9
15	32	6/70–8/70	0	0	0
3	54	8/68–10/68 12/68–3/69	4	6	13

Stream. Both drifters appear to have been influenced by a warm core ring for approximately a week during the middle of this period, so that the length of continuous, unaffected records is quite brief.

Additional limitations are apparent with the remaining drifter data sets as well. The tracks reported by EG&G (1980) are substantially removed to the east of the vicinity of DWD 106 and appear to have occupied positions within the slope water for relatively brief periods. The drifters released in the slope water by Richardson (1981) were also rapidly entrained in the Gulf Stream, remaining within the slope water for less than one month. Finally, the Raytheon data sets (Bisagni, 1981) consisted of positions spaced at intervals of several days to more than a week so that the tracks were too severely aliased to provide information on the relatively high-frequency motion described in the preceding section.

The Lagrangian data remains a significant source of information in the sense that it confirms certain synoptic characteristics of the large-scale slope water circulation which are only weakly implied by the Eulerian records. In particular, the drifter tracks are consistent with a persistent flow pattern directed generally toward the southwest throughout the slope water region. Also, the mean current speeds report by Bisagni (1981) of 16 and 12 cm/sec for the two buoys released at DWD 106 are consistent with the near-surface Eulerian data. This provides support for the presumption that (first-order) current statistics obtained at the upstream mooring locations are representative of DWD 106 and other downstream points within slope water affected by pollutant discharges. Finally, the drifter tracks provide consistent evidence that the general fate of slope water parcels is entrainment within the Gulf Stream. The points of entrainment along the Gulf Stream boundary are scattered, but those drifters which passed close to DWD 106 were uniformly swept into the stream at points east of Cape Hatteras. The residence time within the slope water for pollutants discharged at DWD 106 is presumed to be quite variable, being highly dependent on the extent of warm core ring activity. A best estimate of the mean residence time for the near-surface flow along a track from DWD 106 to the vicinity of Cape Hatteras is on the order of one month.

The drifter tracks do not provide any evidence of a recirculating flow within the slope water region, nor did any of the drifters return to the slope water following entrainment in the Gulf Stream. There is undoubtedly a limited degree of recirculation within the slope water/Gulf Stream system as evidenced by the typical life cycle of warm core rings. However, it would be misleading to compare the complex sequence of circulation events governing the formation and subsequent advection of these rings with a large-scale organized gyre. Also, the degree of recirculation associated with warm core rings is likely to be small so that this mechanism should not be expected to contribute to the long-term accumulation of pollutants within the slope water region.

The possibility of a recirculating gyre cannot be discounted entirely in view of the sparse nature of both the Eulerian and Lagrangian data base within the critical areas of interest along the outer boundary of the slope water region. However, the fact that none of the drifters traced a recirculating pathway does imply that such a circulation feature must be comparatively weak or intermittent.

6. CONCLUSIONS

General circulation in the slope region

A conceptual model representative of the current data analyzed in this report consists of a mean westward-to-southwestward (along-isobath) current extending vertically over the entire depth of the water column and horizontally from the shelf break to the Gulf Stream. Mean currents at certain stations close to the shelf break are not entirely consistent with this general description. However, the record lengths available at these locations are comparatively short, and it is expected that the respective current statistics may be influenced by the locally strong shear effects associated with the dynamics of the shelf/slope front. Over the majority of the slope region, monthly mean speeds may range up to 50 cm/sec at depths above the permanent thermocline (200 meters), but remain within 10 cm/sec below this level. At shallow depths, average speeds rarely exceed 20 cm/sec when computed over record lengths of several months and vector-averaged speeds may be an order of magnitude less.

Superimposed on the mean flow are energetic fluctuations attributable to warm core rings and other perturbations which originate with the dynamic behavior of the Gulf Stream. Near the surface in the presence of warm core rings, low-frequency currents may exceed 100 cm/sec for short durations and 50 cm/sec as monthly averages. Eddy kinetic energy is higher by a factor of 3 to 6 in records that contain warm core ring episodes, as compared with records that reflect only the background currents. Current fluctuations are not found to be highly correlated with seasonal changes or with local wind forcing. This is consistent with previous studies of warm core ring activity in the sense that there is no apparent seasonal effect in the frequency of ring formation or their rate of advection through the slope water region. However, in the absence of rings the current field within the upper 50 meters exhibits an annual variation with an amplitude of 6 cm/sec. This signal becomes negligible at depths greater than 50 meters, implying that an explanation may lie with the low-frequency variability of the wind regime. However, an examination of local wind data does not give strong support to such a relationship. The annual variation may still be attributable to atmospheric forcing in the form of a large-scale wind stress curl which is not well-represented by the single measurement location.

Substantial variability in the profiles of current speed and direction with depth is found at all stations. In general, the vector-averaged speed is found to decrease consistently with depth over the entire water column. In contrast, there does not appear to be a consistent pattern to the depth dependence of current direction. Examples of both clockwise and counterclockwise veering are found at stations in reasonably close proximity. This variability of the vertical current structure is significant because it implies that shear dispersion is an effective mechanism for achieving high dilution rates for dumped wastes.

The horizontal variability of the current field, including the strength of the fluctuations, was examined in detail. As might be expected, gradients of current properties in a direction parallel to the isobaths appear to be negligibly small. This observation is supported by both Eulerian and Lagrangian data sets. An investigation of the cross-isobath variability indicated a weak tendency for the isobath-parallel current component above 200 meters to

increase with distance offshore of the shelf break. The gradient is weak but statistically significant, being estimated at 5 cm/sec per 100 km. A similarly weak tendency was found for the strength of the fluctuations (eddy kinetic energy). The latter may be attributable to the energetic influence of the Gulf Stream along the outer boundary of the slope water region. It is worthwhile to emphasize that the magnitude of these gradients is small and that there is a high degree of scatter in the data. As a first approximation, it remains acceptable to use the long-term statistics gathered from a wide array of station locations to describe the slope circulation in the vicinity of DWD 106.

Circulation at DWD 106

In order to discern further details of the circulation pertinent to waste dispersion processes, progressive vector analyses were performed on several selected near-surface records in the vicinity of Site D. Portions of these records affected by rings were excluded. On the basis of these analyses and inspection of drifter tracks within the slope water, the following results were obtained:

(1) Mean residence time within an area corresponding to the dimensions of DWD 106 is uniformly distributed within a range from one to five days.

(2) Short-term stagnation periods of at least five days duration, during which the virtual displacement is less than the dimension of DWD 106, have an incidence of between 17% and 31%.

(3) The incidence of current episodes below 5 cm/sec is on the order of 10%, and the mean persistence of such events is typically less than two days.

(4) Periods of on-shelf motion are infrequent, with an incidence of roughly 15%.

(5) On-shelf displacements occur at rates that could carry wastes to the outer portions of the continental shelf within a period of several days.

(6) Short-term recirculation events which would return wastes to the area of DWD 106 within periods of a few weeks or less are rare.

(7) The longer-term fate of wastes dumped at DWD 106 appears to be entrainment by the Gulf Stream within a period of roughly one month, with little likelihood of subsequent large-scale recirculation to the slope water region.

References

Bisagni, J.J. 1976. Passage of anticyclonic Gulf Stream eddies through Deep-water Dumpsite 106 during 1974 and 1975. NOAA Dumpsite Evaluation Report 76-1, Washington, D.C.

Bisagni, J.J. 1981. Lagrangian measures of advection of near-surface waters at the 106-Mile dumpsite. NOAA Technical Memorandum OMPA-11. Boulder, Colorado.

Boicourt, W.C. 1973. The circulation of water on the continental shelf from Chesapeake Bay to Cape Hatteras. Ph.D. Thesis. The Johns Hopkins University, Baltimore, MD.

Beardsley, R.C. and C.D. Winant. 1979. On the mean circulation in the mid-Atlantic Bight. J. Phys. Oceanogr., 9:612-619.

Bumpus, D.F. 1976. Review of the physical oceanography of Georges Bank. International Commission for the Northwest Atlantic Fisheries Research, Bulletin, 12:109-134.

Butman, B. and R.C. Beardsley. 1984. Long term observations on the southern flank of Georges Bank; seasonal cycle of currents. Submitted to J. Phys. Oceanogr.

Clarke, R.A., H. Hill, R.F. Reinger, and B.A. Warren. 1980. Current system south and east of the Grand Banks of Newfoundland. J. Phys. Oceanogr., 10:25-65.

Csanady, G.T. and P.T. Shaw. 1983. The "insulating" effect of a steep continental slope. J. Geophys. Res., 88:7519-7524.

Csanady, G.T. 1977. The coastal jet conceptual model in the dynamics of shallow seas. In: Goldberg, E.D., I.N. McCave, J.J. O'Brien, and J.H. Steele (eds.) The Sea, Vol. 6, J. Wiley, New York. pp. 117-144.

EG&G. 1982. Interpretation of the physical oceanography of Georges Bank. Report submitted to the Bureau of Land Management, Washington, D.C. by EG&G, Environmental Consultants, Waltham, Massachusetts.

EG&G. 1981. Review of the oceanography of submarine canyons off the east coast of the United States. (Unpub.) Report submitted to the American Petroleum Institute.

EG&G. 1980. Data Report: Lagrangian Studies August-December 1979. Appendix A of Thirteenth Quarterly Progress Report, New England Outer Continental Shelf Physical Oceanography Program. Report submitted to the Bureau of Land Management, New York OCS Office.

EG&G. 1978. Analysis report: Interaction of a Gulf Stream eddy with Georges Bank. Appendix D of the Eighth Quarterly Progress Report, New England Outer Continental Shelf Physical Oceanography Program. Report submitted to the Bureau of Land Management, New York OCS Office.

Fairbanks, R. G. 1982. The origin of continental shelf and slope water in the New York Bight and Gulf of Maine: Evidence from $H_2{}^{18}O/H_2{}^{16}O$ ratio measurements. J. Geophys. Res., 87:5796-5808.

Flagg, C.N. 1984. The hydrographic structure and variability of Georges Bank. Chapter 4.3 In: Backus, R. (ed.) Georges Bank, MIT Press.

Flagg, C.N. 1977. The kinematics and dynamics of the New England Continental Shelf and shelf/slope front. Ph.D. thesis, Massachusetts Institute of Technology/Woods Hole Oceanographic Institution, Joint Program, Woods Hole, Massachusetts. 207 pp.

Fofonoff, N.P. and H. Bryden. 1975. Specific gravity and density of sea water at atmospheric pressure. J. Mar. Res., 33 (Supplement).

Fuglister, F.C. 1963. Gulf Stream '60. Progress in Oceanogr., 1: 265-373.

Gatien, M.G. 1976. A study in the slope water region south of Halifax. J. Fish. Res. Board Can., 33:2213-2217.

Gotthardt, G.A. and G.J. Potocsky. 1974. Life cycle of a Gulf Stream anti-cyclonic eddy observed from several oceanographic platforms. J. Phys. Oceanogr., 41:131-134.

Halliwell, G. and C. Mooers. 1979. The space-time structure and variability of the shelf water-slope water and Gulf Stream surface temperature fronts and associated warm core eddies. J. Geophys. Res., 84:7707-7725.

Hamilton, P. 1982. Analysis of current meter records at the Northwest Atlantic 2800 metre radioactive waste dumpsite. U.S. Environmental Protection Agency, Washington, D.C., EPA 520/1-82-002.

Hansen, D.V. 1970. Gulf Stream meanders between Cape Hatteras and the Grand Banks. Deep Sea Res., 17:495-511.

Hogg, N. 1981. Topographic waves along 70°W on the continental rise. J. Mar. Res., 39:627-649.

Iselin, C.O. 1936. A study of the circulation of the western North Atlantic. MIT/WHOI Pap. Phys. Oceanogr. and Meteor., 4(4):1-101

Kester, D. 1981. Interdisciplinary study of warm core ring physics, chemistry, and biology. Project Overview, March.

Kroll, J. and P.P. Niiler. 1976. The transmission and decay of topographic Rossby waves incident on a continental shelf. J. Phys. Oceanogr., 6:432-450.

Lai, D.Y. and P.L. Richardson. 1977. Distribution and movement of Gulf Stream rings. J. Phys. Oceanogr., 7:670-683.

Luyten, J.R. 1977. Scales of motion in the deep Gulf Stream and across the continental rise. J. Mar. Res., 35:49-74.

McLellan, H.J. 1957. On the distinctness and origin of the Slope Water off the Scotian shelf and its easterly flow south of the Grand Banks. J. Fish Res. Bd. Can., 14(2), pp. 213-239.

Morgan, C.W. and J.M. Bishop. 1977. An example of Gulf Stream eddy-induced water exchange in the mid-Atlantic Bight. J. Phys. Oceanogr., 7:472-479.

Ou, H.W. 1980. On the propagation of free topographic Rossby waves near continental margins. Part I: Analytical model for a wedge. J. Phys. Oceanogr., 10:1051-1060.

Ou, H.W. and R.C. Beardsley. 1980. On the propagation of free topographic Rossby waves near continental margins. Part II: Numerical model. J. Phys. Oceanogr., 10:1323-1339.

Rhines, P.B. 1971. A note on long-period motions at Site D. Deep Sea Res., 18:21-26.

Rhines, P.B. 1970. Edge-, bottom-, and Rossby waves in a rotating stratified fluid. Geophys. Fluid Dyn., 1:273-302.

Richardson, P. L. 1981. Gulf Stream trajectories measured with free drifting Buoys. J. Phys. Oceanogr., 11:999-1010.

Richardson, P.L. 1977. On the crossover between the Gulf Stream and the Western Boundary Undercurrent. Deep Sea Res., 24:139-159.

Saunders, P.M. 1971. Anticyclonic eddies formed from shoreward meanders of the Gulf Stream. Deep Sea Res., 18:1515-1219.

Schroeder, E.H. 1966. Average monthly temperatures in the North Atlantic Ocean. Deep Sea Res., 12:323-343.

Schroeder, E.H. 1963. North Atlantic temperatures at a depth of 200 meters. Amer. Geogr. Soc. Serial Atlas of the Marine Environment, Folio 2.

Scott, J.T. and G.T. Csanady. 1976. Nearshore currents off Long Island. J. Geophys. Res., 81:5401-5409.

Semtner, A.J. and Y. Mintz. 1977. Numerical simulation of the Gulf Stream and mid-ocean eddies. J. Phys. Oceanogr., 7:208-230.

Smith, P.C. 1978. Low-frequency fluxes of momentum, heat, salt, and nutrients at the edge of the Scotian shelf. Journal of Geophysical Research, 83:4079-4096.

Smith, P.C. and B.D. Petrie. 1982. Low-frequency circulation at the edge of the Scotian Shelf. J. Phys. Oceanogr., 12:28-46.

Spencer, A. 1979. A compilation of moored current meter data and associated oceanographic observations, Volume XX (Rise Array, 1974). Woods Hole Oceanographic Institution Tech. Rpt. WHOI 79-56, Woods Hole, Massachusetts.

Swallow, J.C. and L.V. Worthington. 1961. An observation of a deep counter-current in the western North Atlantic, Deep Sea Res., 8:1-19.

Swallow, J.C. and L.V. Worthington. 1969. Deep currents in the Labrador Sea. Deep Sea Res., 16:77-84.

Tarbell, S., M. Chaffee, A. Williams, and R. Payne. 1980. The WHOI Moored Array Project, 1963-1978: Data directory and bibliography. Woods Hole Oceanographic Institution Tech. Rpt. WHOI 79-88, Woods Hole, Massachusetts.

Tarbell, S. and A.W. Whitlach. 1977. A compilation of moored current data and associated oceanographic oberservations, Volume XV (1971 measurements). Woods Hole Oceanographic Institution Tech. Rpt. WHOI 77-56, Woods Hole, Massachusetts

Thompson, R. 1978. Reynolds stress and deep counter-currents near the Gulf Stream. J. Mar. Res., 36:611-615.

Warren, B.A. 1981. Deep circulation of the world oceans. In: Warren, B.A. and C. Wunsch (eds.) Evolution of Physical Oceanography. MIT Press, Cambridge, Massachusetts.

Webster, F. 1969. Vertical profiles of horizontal ocean currents. Deep Sea Res., 16:85-98.

Wright, W.R. 1977. Environmental Inventory of the North Atlantic Continental Slope; Chapter 4, Physical Oceanography. Report by the Research Institute of the Gulf of Maine, submitted to the Bureau of Land Management, Department of Interior.

Wunsch, C. and R. Hendry. 1972. Array measurements of the bottom boundary layer and the internal wave field on the continental slope. Geophys. Fluid Dyn., 4:101-145.

Acknowledgements

This report was prepared by EG&G WASC Oceanographic Services for the National Oceanographic and Atmospheric Administration under Contract No. NA82RAD00006. Principal Investigators were Dr. Charles Flagg and Mr. Daniel Frye. Mr. Peter Daifuku performed all computer analyses of the moored current data. Mr. John Borchardt, Dr. Scott McDowell and Mr. William Galen also participated in the report preparation. Special appreciation is extended to Dr. Robert Beardsley (WHOI), Dr. Mario Viera (SUNY), and Dr. George Heimerdinger (NODC) for their assistance in providing the raw data records; and to the many members of the WHOI Buoy Group.